Liquid Film Migration in an Al-3.6 wt% Cu alloy

By

G.V.S.N. Raja Sekhar

DEPARTMENT OF MATERIALS AND METALLURGICAL ENGINEERING

INDIAN INSTITUTE OF TECHNOLOGY KANPUR

JANUARY, 2004

Liquid Film Migration in an Al-3.6 wt% Cu alloy

A thesis submitted

in the partial fulfilment of the requirements

for the Degree of

Master of Technology

by

G.V.S.N. Raja Sekhar

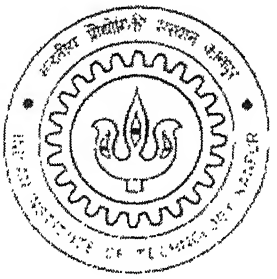

to the

Department of Materials and Metallurgical Engineering

INDIAN INSTITUTE OF TECHNOLOGY, KANPUR

January, 2004

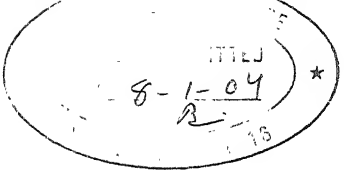

CERTIFICATE

This is to certify that the work contained in the thesis entitled "**Liquid Film Migration in an Al-3.6 wt% Cu alloy**" by G.V.S.N. Raja Sekhar has been carried out under my guidance and that this work has not been submitted elsewhere for a degree.

Dr. S.P. Gupta

Department of Materials and Metallurgical Engineering,

Indian Institute of Technology,
Kanpur.

Jan., 2004

ACKNOWLEDGEMENT

At the outset, I would like to express my deepest regards and most sincere gratitude to my teacher and thesis supervisor Dr. S. P. Gupta for his earnest involvement, active guidance and impetus, without which this work could not have seen the light of day. His inspiration and support made my work successful.

I wish to thank my lab mates chinta babu and suresh whose company made me enjoyable to work with them.

I would like to thank Dr. Mungole, rajan and Chandra sekhar for their constant cooperation in completion of my thesis.

I would like to thank my friends mallik, satish, pk, nagaraj, anand, murthy, ravi, sahana, sankar, surender, imam, manoj, anil, sridevi and pavani whose company made my stay at iitk a memorable one.

G.V.S.N. Raja Sekhar

Indian Institute of Technology, Kanpur

January, 2004

ABSTRACT

Liquid Film Migration (LFM) in an Al-3.6 wt% Cu alloy during isothermal annealing after down and up-quenching from an equilibrated state at 615°C in the α+liquid phase field has been studied. A change in the equilibrated state caused by an abrupt change in temperature resulted in liquid films migrating against their curvature from one grain into another leaving behind alloyed or dealloyed zones in down and up-quenching experiments respectively. The migration distance, x, for both down and up-quenching treatments was observed to decrease monotonically with annealing time, t, and has been observed to obey a power law relationship, $x = kt^n$, with annealing time. The exponent n falls in the range 0.20 and 0.25. The coherency strain energy developed in the grain being consumed does not seem to be large enough to drive the reactions against the curvature observed. The solute concentration gradient across the migrating liquid film, ΔX_B, has been calculated to be of the order of 10^{-4}. The mass balance equation (Fick's law) was used to calculate the diffusion coefficient from growth rate, v, the composition difference, ΔX_B, thickness of the liquid film, δ, radius of curvature, r, and the distribution coefficient, k. The diffusion coefficients in the down-quenching experiment have been observed to be in the range 0.783×10^{-9} to $1.534\times10^{-9} m^2s^{-1}$. Similarly, the diffusion coefficients in the up-quenching experiment have been observed to be in the range 1.729×10^{-8} to $1.905\times10^{-8} m^2s^{-1}$. These values lie well within the diffusion coefficients of self diffusion of liquid aluminium and liquid copper suggesting that, the liquid film migration during down and up-quenching treatments was controlled by the diffusion of solute through the liquid film

Contents

List of Figures

List of Tables

1. INTRODUCTION

The liquid films between grains in alloys equilibrated in solid-liquid phase fields have been observed to migrate with simultaneous changes in the compositions behind them is known as Liquid Film Migration (LFM). This phenomenon was first reported by Yoon and Huppmann [1] during the liquid-phase sintering of tungsten with liquid nickel. Pure tungsten grains initially in contact with pure liquid nickel were first dissolved and then reprecipitated as a solid solution saturated with nickel. The process had the appearance of the intrusion of a liquid film, which initially separated the tungsten grains, into the dissolving grain, while the growing grain formed by the deposition of equilibrium W-Ni solid solution. It has been observed to occur in a variety of metallic systems [2], oxides [3] and compounds under various conditions i.e. during solute diffusion, partial melting, in the heat affected zones of weldments [4] and isothermal heat treatment of systems of two phases which are not in equilibrium.

In all the above cases it was found that the liquid films often migrated against their mean radii of curvature, indicating that the migration could not have been driven by capillary effects. The phenomenon of LFM is similar to Chemically Induced Grain Boundary Migration (CIGM or DIGM) in polycrystalline solids, in which grain boundaries experience a diffusional flux along their length, and migrate into one of the parent grains, depositing a solid solution of altered composition in their wake. In both processes, there is clearly a persistent driving force, which is capable of moving interfaces, often against their curvature, and leaves a new solid solution in the region swept by the migrating interface.

1.1 Theories

The diffusional coherency strain theory was first proposed by Sulonen [5] in 1957 by observing that discontinuous precipitation (DP) only seemed to occur in systems exhibiting at least 10% difference in atomic size, and proposed that during DP, lattice diffusion ahead of moving grain boundaries could create a composition variation over a thin layer that was coherent with the parent lattice, and the resulting strain energy was the driving force. In 1972, Hillert [6] following the Sulonen's proposal, analyzed the effect of coherency strain energy in the frontal diffusion zone on discontinuous precipitation and in view of the similarity between the discontinuous precipitation and

DIGM, he suggested that the same coherency strain energy could also drive LFM. Yoon et al [7] and Handwerker et al [8] developed this argument further for the case of LFM. They used the thermodynamic analysis of self-stress in a crystalline solid developed by Larché and Cahn [9] to define the boundary conditions for diffusion of solute across the liquid film. Then, invoking the condition of local equilibrium, they were able to develop an approximate expression for the rates of LFM in binary systems.

The process of LFM is often visualized by considering the states of two grains separated by a liquid film. The surfaces of the two grains are each considered to be in equilibrium with the liquid phase. If the stresses in these adjacent grains are different such that the liquids in equilibrium with these grains have different compositions, a composition gradient will exist across the liquid film, which in turn leads to diffusion, and migration of the liquid film.

The effect of a coherency strain field caused by a solute concentration gradient in a solid phase was first studied in depth by Cahn [10] in his treatment of spinodal decomposition. He included a strain energy term in the total Helmholtz free energy expression, the extra free energy arising from the fact that the molar volume of a solid is generally a function of composition. As a result there is an energy increase where adjacent regions of different composition and thus lattice parameter are coherently connected. For cubic crystals, under the assumptions of linear elasticity and linear variation of lattice parameter with concentration, the local elastic strain energy per unit volume is given by

$$w_{el} = Y(\hat{n})(C_s - C_o)^2 \eta^2 \qquad (1)$$

where $Y(\hat{n})$ is an orientation dependent biaxial elastic modulus, $\hat{n}$ is a unit vector representing the normal of the biaxially stressed plane and C_s and C_o are the local and average concentrations of solute, respectively. η is a measure of the solute misfit.

With the above prescription for the local strain energy density, it is possible to develop a thermodynamic description of LFM. This was done by Hillert [11] who considered a liquid film separating two grains, and assumed a thin layer of a different composition to be coherent with a parent grain of composition C_o. He assigned to material in this layer an extra molar free energy due to coherency given by $V_m \times W_{el}$, where V_m is a molar volume and W_{el} is given by equation (1). Figure 1.1 shows the molar free energy diagram for a binary system in which a thin stressed α layer,

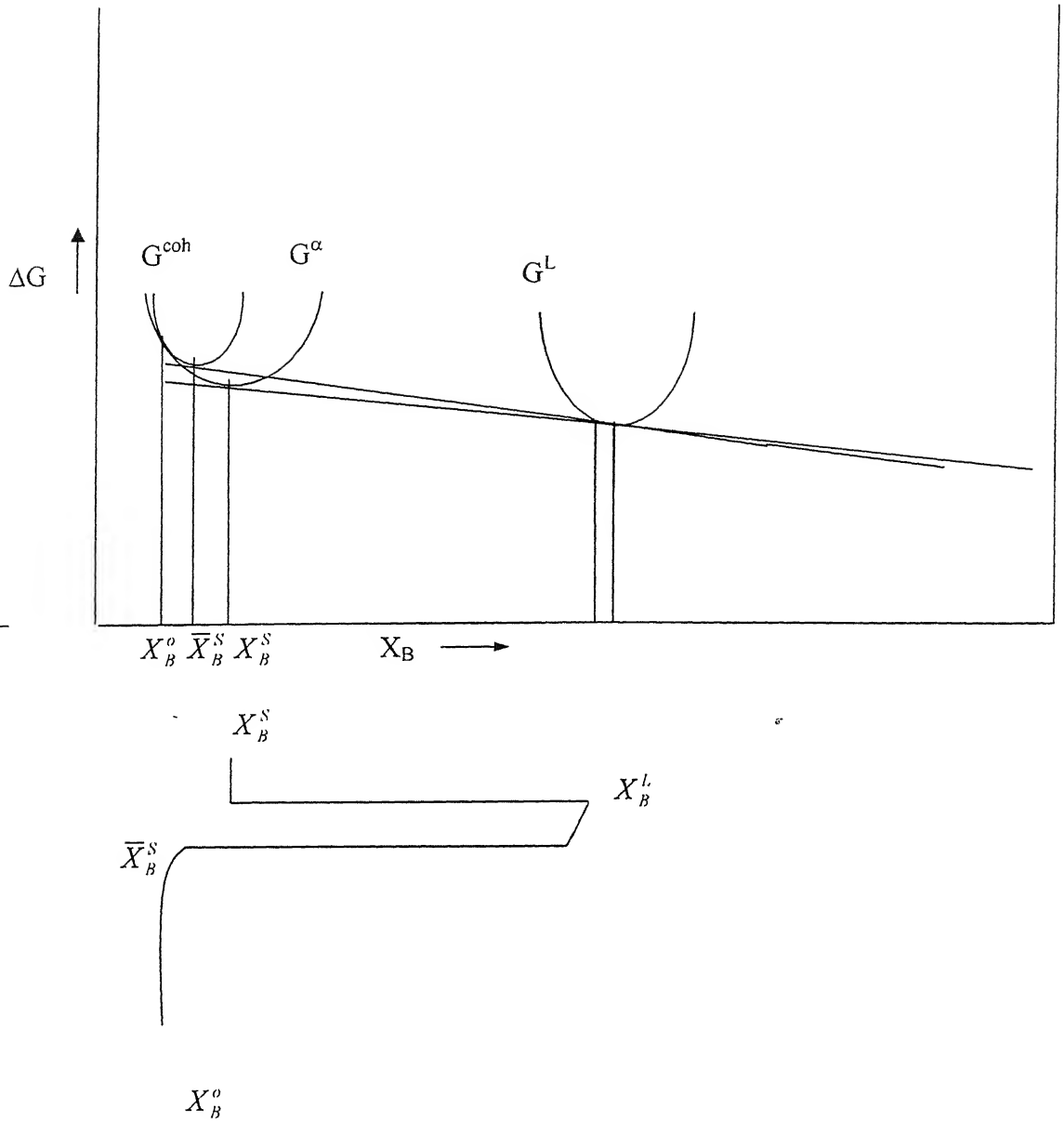

Fig. 1.1. Coherent and stress-free solid-liquid equilibria, as they apply to the migration of a planar liquid film: The parent phase solid composition is X_B^o. The lower part of the figure is a schematic concentration profile across the liquid film.

coherent with a large α grain, is in equilibrium with a B-rich liquid phase. The equilibrium compositions are obtained from a common tangent construction. Hillert then derived the driving force ΔG for transfer of material from the coherent layer to a stress-free α phase assuming ideal solution behavior, and obtained ΔG equal to the coherency strain energy. The corresponding graphical construction is shown schematically in Fig.1.1 and represents the free energy curves of coherently strained

solid and unstrained solids, assumed to be in equilibrium with a B-rich liquid, and the accompanying concentration profile that develops across the liquid film.

Larché and Cahn [9] derived the relevant equilibrium conditions from the thermodynamics of solids for the case of a dilute, binary solution, with a stressed and curved solid in equilibrium with the liquid and for an unstressed and planar solid in equilibrium with the liquid. Their results implied that the Gibbsian common tangent construction is valid for both cases.

1.2 Driving Force

An expression for the net thermodynamic driving force, free energy change per unit distance of reaction front migration per unit area of reaction front, for the migration of reaction fronts during diffusion induced grain boundary migration (DIGM), discontinuous precipitation (DP) and liquid film migration (LFM) in binary alloys has been derived recently by Fournelle [12] from a two-dimensional model which considers individual segments of the migrating reaction front as open systems which can receive solute and solvent atoms from or give them up to the surrounding material.

The overall free energy change ΔG associated with the migration of the reaction front by a distance L_o is given by

$$\Delta G = G_1\text{-}(G_o + G_A + G_B)$$

Where G_1 is the free energy of the volume left behind as a differential segment of boundary migrates through distance L_o, G_o is the free energy of the volume swept through and G_A and G_B are associated with any A or B atoms being gained from or lost to the surrounding material.

$$G_1 = \frac{G^b}{V^b}(\delta dyw) + \frac{G^1}{V^1}(L_1 dyw)$$

$$G^o = \frac{G^b}{V^b}(\delta dyw) + \frac{G^0}{V^0}(L_0 dyw)$$

$$G_A = \left\{ J_A - \left(J_A + \frac{\partial J_A}{\partial y} \right) \right\} \overline{G}_A^b \delta w \Delta t$$

and

$$G_B = \left\{ J_B - \left(J_B + \frac{\partial J_B}{\partial y} dy \right) \right\} \bar{G}_B^b \delta w \Delta t$$

here, G^l,G^o and G^b and V^l, V^o and V^b are the molar free energies and volumes respectively of the growing grain, retreating grain and reaction front, L_o and L_1 are the distances swept through and left behind by the reaction front respectively, J_A and J_B are the fluxes of A and B atoms along the reaction front respectively, $\bar{G}_A^b$ and $\bar{G}_B^b$ are the partial molar free energies of the A and B atoms entering and leaving the volume element via the reaction front respectively, δ is the thickness of the liquid film, w is the width of the foil and Δt is the time for the reaction front to migrate a distance L_o. The overall free energy change per unit distance of migration per unit area of reaction front in terms of the thermodynamic properties is given as

$$\Delta G = \frac{1}{V_o} \left\{ \left(G^l - G^o \right) - \left(X_{Cu}^l - X_{Cu}^o \right) \times \left[\frac{\left(G^l - \bar{G}_{Al}^l \right) D_{Al}^l - \left(G^l - \bar{G}_{Cu}^l \right) D_{Cu}^l}{X_{Cu}^l D_{Al}^l + X_{Al}^l D_{Cu}^l} \right] \right\} \qquad (2)$$

here, V_o is the molar volume, G^l is the molar free energy of the alloyed or dealloyed grain left behind the migrating liquid film, G^o is the molar free energy of the grain in front of the liquid film, X_{Cu}^l and X_{Al}^l are mole fractions of Cu and Al in the alloyed or dealloyed grain, X_{Cu}^o is the mole fraction of Cu in the grain in front of the boundary, and D_{Cu}^l and D_{Al}^l are the diffusivities of Cu and Al in the liquid film or grain boundary.

In the above equation the first term describes the molar free energy difference between the growing grain and the grain being consumed. The second term describes the free energy change associated with the atoms gained or lost from the system as the result of diffusion along the liquid film.

Free energy change for the present investigation can be calculated using equation (2). Values of G^l, G^o were calculated by the equation

$$\begin{aligned} G^i = {} & F_{Al}^i (1 - X_B) + F_{Cu}^i X_B + RT \left[X_B \ln X_B + (1 - X_B) \ln (1 - X_B) \right] \\ & + X_B (1 - X_B) \left[B^i + C^i (1 - 2X_B) \right] \end{aligned} \qquad (3)$$

given by Murray [13]. Where i designate the phase, X_B is the atom fraction of Cu, F^i is the Gibbs energies of the pure metals, and B^i and C^i are the temperature dependent

interaction parameters. F_{Al}^{i} and F_{Cu}^{i} can be calculated from the equations (4) to (7), given by Kaufman and Nesor [14].

$$F_{fcc(Al)} = -10711 + 11.506T \quad (4)$$

$$F_{fcc(Cu)} = -13054 + 9.623T \quad (5)$$

$$B_{fcc} = -45417 + 0.565T \quad (6)$$

$$C_{fcc} = -38681 - 1.276T \quad (7)$$

Using equations (3) to (7), Free energy vs. Composition curves can be drawn at each temperature and tangent drawn at X_{Cu}^{l} to obtain the corresponding $\bar{G}_{Al}^{l}$ and $\bar{G}_{Cu}^{l}$.

The values of the Cu diffusivities D_{Cu}^{l} in the liquid films can be determined from the parameters $D_o = 8.1\times10^{-7}$ m^2s^{-1} and Q=38.9 kJ mol^{-1} given by Owadano et al [15]. The values for D_{Al}^{l} can be calculated from the following equation given by Gjostein [16].

$$D_{Al}^{l} = 2.3\times10^{-7}\exp\left(\frac{-Q}{RT}\right)m^2s^{-1}$$

Calculation can also be carried out to determine the coherency strain energy as the driving force for comparison by using following equation as given in reference [11]

$$\Delta G_{coh} = \frac{E\eta^2 V_m (X_B^{\alpha} - X_B^{o})^2}{1-\nu} \quad (8)$$

where, E is the modulus of elasticity, η the misfit parameter, X_B^{α} and X_B^{O} are the compositions in the grain in front of the migrating grain boundary and well away from it respectively and ν is the Poisson's ratio.

The driving force for the present investigation was also calculated by the equation given below for the purpose of comparison, as given in reference [17]

$$\Delta G = \frac{-\frac{1}{2}RT\left(X_B^{\alpha} - X_B^{o}\right)^2}{X_B^{o}} \quad (9)$$

1.3 Phase diagram:

The phase diagram of Al-Cu system is shown in Fig.1.2. Based on the phase diagram the composition of the alloy and the treatment temperatures were selected. From the phase diagram we can see that Cu solubility in Al increases with temperature up to the eutectic temperature i.e. 548°C. The maximum solubility of Cu in Al at eutectic temperature is 5.4 wt%. The alloy used in the present investigation has 3.6wt% Cu and this is in single-phase field (α) at the eutectic temperature. The

solidus temperature for the present alloy is approximately 590°C. The temperatures are so selected that, the alloy is recrystallized in single-phase field and homogenized in α+liquid field.

System, Solvent-(solute)	Mode	Specimen Geometry	Temperature, °C
Co-(Cu)	LFM	Liquid phase sintering (LPS)	1150 (T down)
Cu-(Cd)	LFM	Bulk	510-550 (down)
Cu-(In)	LFM	Bulk	T_s + 8,10°C (up)
Cu-(Ni)	LFM	Bulk	T_s + (T up)
Incoloy 903	LFM	Bulk	Room
Mo-(Ni)	LFM	LPS	1390 (down)
Mo-Ni-(Fe)	LFM	LPS	1400
M0-Ni-(W)	LFM	LPS	1380-1450
Ni base superalloy	LFM	Bulk	1204
Ni alloy 718	LFM	Bulk	1227
Sb-(Bi)	LFM	Bulk	T_s+(12-70) (T up)
Sb-(Sn)	LFM	Bulk	T_s+(T up)
TiC-Fe-(Fe)	LFM	Bulk	1470
W-(Ni)	LFM	Powder	1640
ZrO_2-(Y_2O_3)	LFM	Bulk	1250-1400
ZrO_2-(CeO_2)	LFM	Bulk	Room (down)
$SrTiO_3$-Nb_2O_3-(Cao.Bao)	LFM	Bulk	1100-1400

Table 1.1. Some material systems exhibiting liquid film migration. [18]

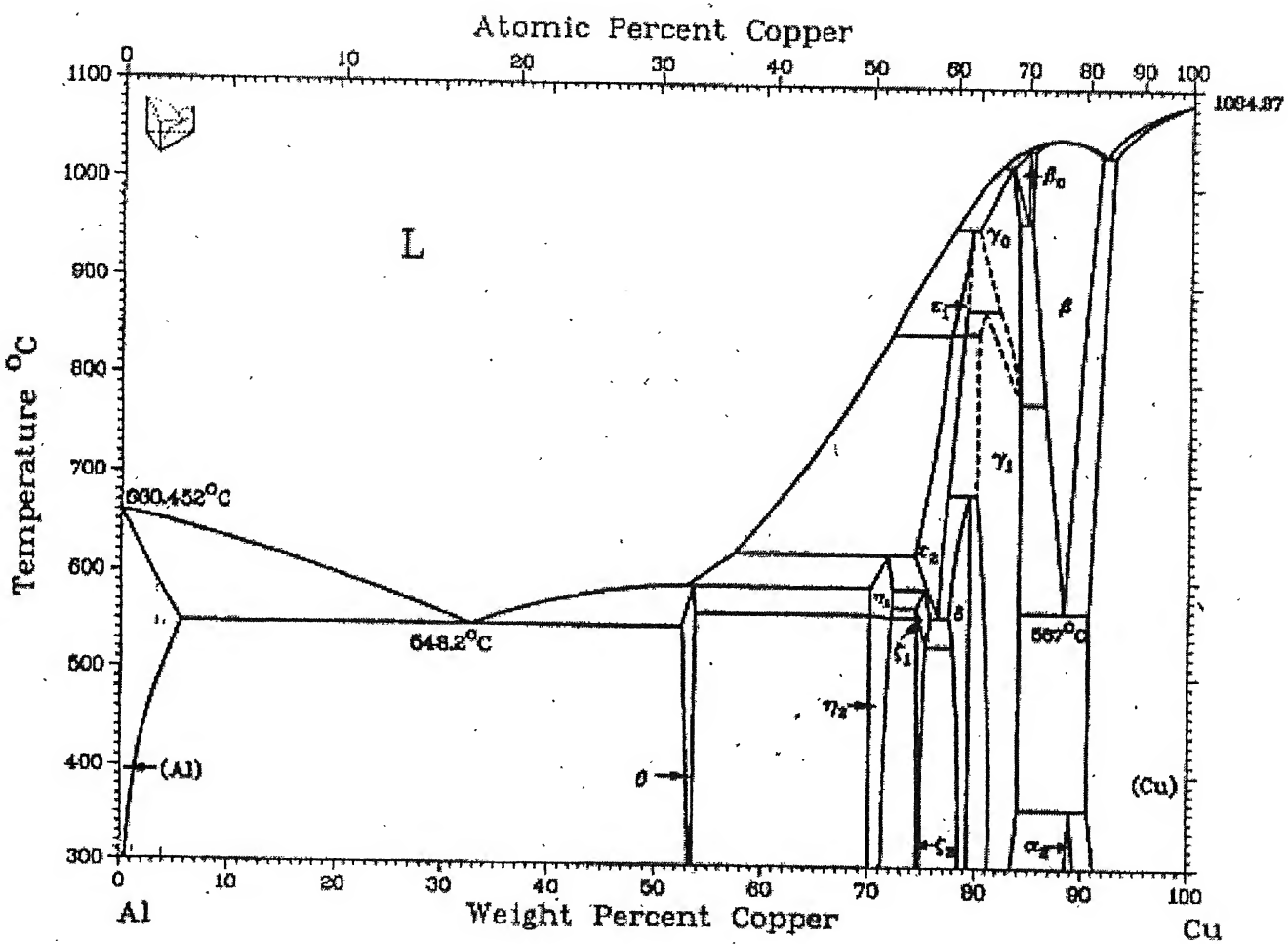

Fig.1.2. Phase diagram of Al-Cu alloy system.

2. Experimental procedure

The Liquid film migration in an Al- 3.6 wt% Cu alloy has been studied in the present investigation. The alloy was prepared from Al and Cu both of 99.99% purity. An Al-50 wt% Cu master alloy was melted in an alumina crucible encapsulated in quartz tube under vacuum of 10^{-3} atm. The alloy was prepared by adding pure Al in measured amount and melting in a graphite crucible under argon atmosphere. It was cast in split graphite molds of 11mm internal diameter. These ingots were sealed in quartz capsule under vacuum of 10^{-3} atm. and subsequently annealed for one week at 550^0C in a tubular furnace. All ingots were quenched in ice plus water mixture after homogenization. They were cut to 5 mm thick slices followed by cold rolling to 1 mm thick sheets. The sheets were then cut into 6mm×6mm specimens in a diamond cutter. The samples were cleaned ultrasonically to ensure that the oil traces and dirt deposited while cutting were removed. The individual samples were encapsulated in quartz tubes under vacuum.

Each specimen was recrystallized at 530^0C for 1 hr to get a grain size of the order of 500 μm. All samples were transferred to another tubular furnace maintained at 615^0C and treated for 12 hours to form liquid layer on the grain boundaries. The specimens were then immediately transferred to another tubular furnace controlled within $\pm 2^0$C in the temperature range from 500 to 647^0C in order to cause LFM. After the treatment each specimen was quenched in ice plus water mixture. A number of specimens were treated at each temperature for different durations.

The specimens were then ground and polished through 0.05 μm Al_2O_3 using standard metallographic techniques. They were etched with Keller's reagent (2 ml HF, 3ml HCl, 5 ml HNO_3 and 190 ml H_2O) and examined under an optical microscope. The migration distance of the liquid film was measured from its initial position with the help of a reticule fitted in the optical microscope. At least 40 data points were recorded from each specimen and the data averaged. The thickness of the liquid film was also measured using the same reticule. The microstructure was recorded through a digital camera fitted with an image analyzer.

3. Results and Discussion

3.1 The microstructure developed during liquid film migration in the up-quenched and down-quenched specimens will be described in this section.

Fig.3.1 is a microstructure showing LFM that occurred when an Al-3.6wt% Cu alloy sample is down quenched to 580°C in the single-phase field from 615°C and held for 5 s. The liquid films are observed to be bulging out indicating the start of migration. As the time given for migration was just 5 s, the liquid formed during annealing at 615°C still persists and very small amount of it has been consumed. The second phase visible in the microstructure is the liquid globules formed in the grain during annealing and is retained after quenching. Examination at higher magnification shows that the former liquid regions are now either θ phase for the smaller regions (thin films) or a eutectic mixture of α and θ phases for the larger regions (triple points).

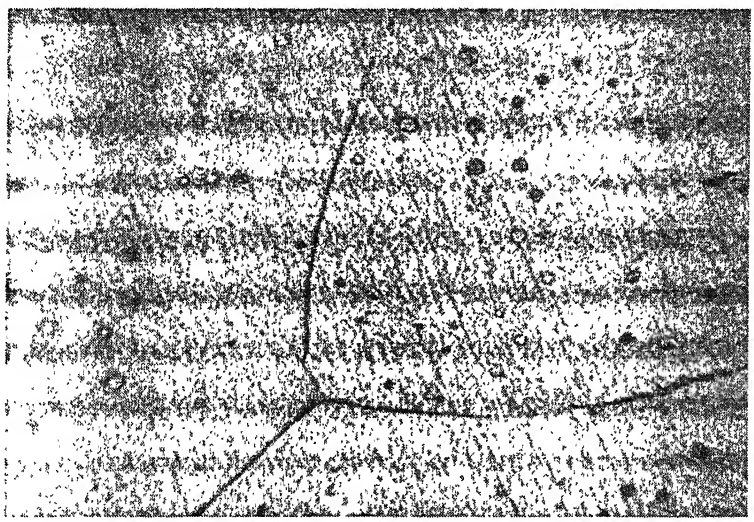

Fig.3.1. The microstructure of Al-3.6wt% Cu alloy, annealed at 615°C in the α+liquid field for 12 h and then down-quenched to 580°C in the α phase field and held for 5 s. Magnification 200X

Fig.3.2 is a microstructure showing LFM that has occurred when the alloy sample is down quenched to 580°C and held for 10 s. The migration distance has increased with time. The triple points as well as the neighboring liquid layer on the boundary act as the source of solute. The regions formed behind the migrating grain boundary are expected to be enriched by solute. The liquid has still not exhausted.

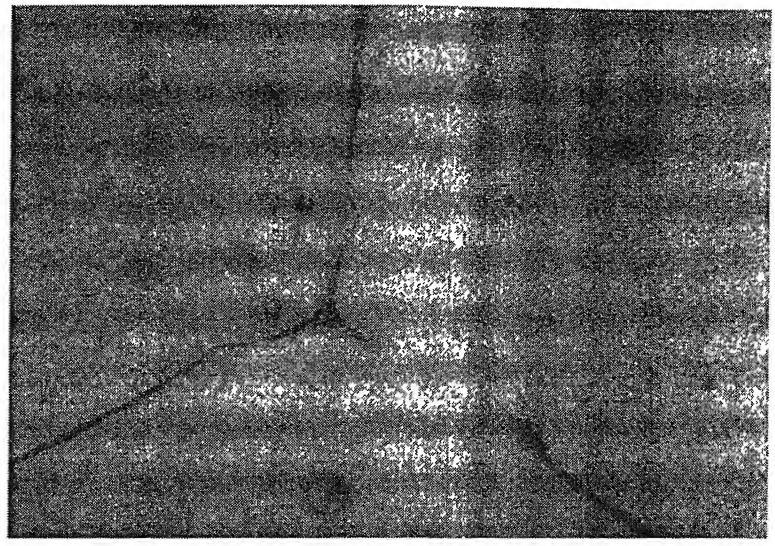

Fig.3.2. The microstructure of Al-3.6wt% Cu alloy, annealed at 615°C in the α+liquid field for 12 h and then down-quenched to 580°C in the α phase field and held for 10 s. Magnification 200X.

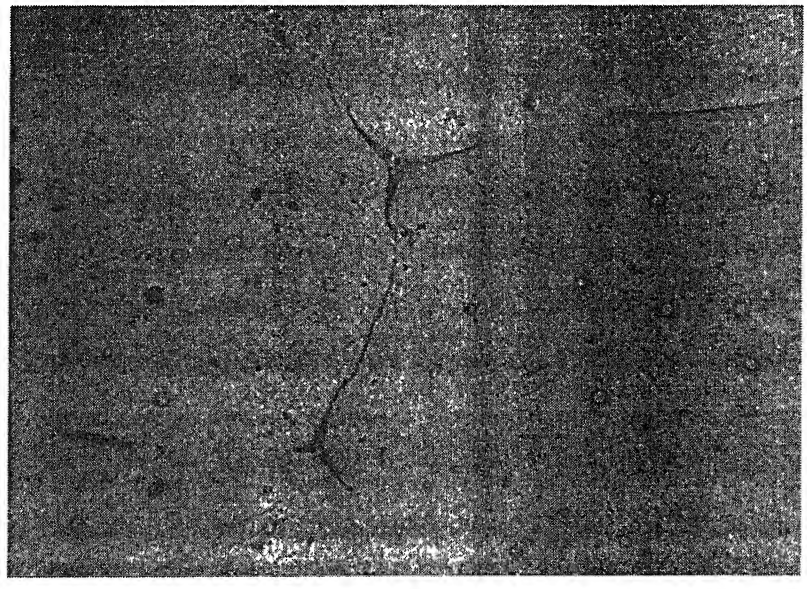

Fig.3.3. The microstructure of Al-3.6wt% Cu alloy, annealed at 615°C in the α+liquid field for 12 h and then down-quenched to 580°C in the α phase field and held for 20 s. Magnification 200X.

Fig.3.3 is a microstructure showing the LFM that has occurred when the sample is down quenched to 580°C and held for 20 s. The migration distance and the radius of curvature of the grain boundary are observed to be increasing with time. It has been observed that the amount of liquid in the film has been consumed gradually as the migration progresses. It is observed that the migrating liquid film does not maintain spherical shape in this system, i.e. curvature is not maintained as the time passes and

boundary becomes flat. The drag experienced by the migrating liquid film or reversal of the direction of migration in a segment of the migrating front may be the reason for this type of behavior.

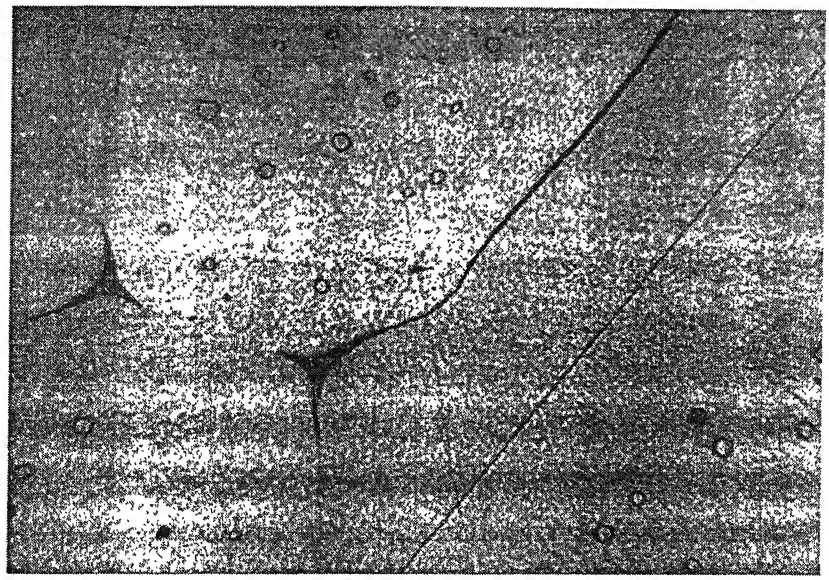

Fig.3.4. The microstructure of Al-3.6wt% Cu alloy, annealed at 615°C in the α+liquid field for 12 h and then down-quenched to 580°C in the α phase field and held for 40 s. Magnification 200X.

Fig 3.4&3.5 are microstructures showing the DIGM that has occurred when samples are down quenched to 580°C and held for 40 s and 90 s respectively. The thickness of liquid film has been observed to decrease as the time of transformation increases. The migration distance has increased with time and front portion of the curved liquid film does not show a proper contrast at some boundaries. It is due to the insufficient supply of solute from triple points and also from adjacent thick liquid film from which it has bulged out. The low solute diffusivity and higher solute drag might be the reasons for this type of behavior in addition to the reversal of direction in a segment of the migrating film. The initial position of the liquid film is not visible in any of the photograph.

Fig.3.6 is the microstructure showing LFM that has occurred when the sample is down quenched to 580°C and held for 3 min. The liquid film has become a grain boundary at some segments. The migrating liquid film has lost its curvature and become flat forming low angle grain boundary, which has low mobility for such boundaries. The mobility of grain boundary mainly depends on a number of factors such as misorientation angle, density of dislocations, vacancies, extent of segregation, etc. In

general high angle grain boundaries have higher mobility and therefore migrate faster in comparison to low angle boundaries or boundaries in coincidence site orientation.

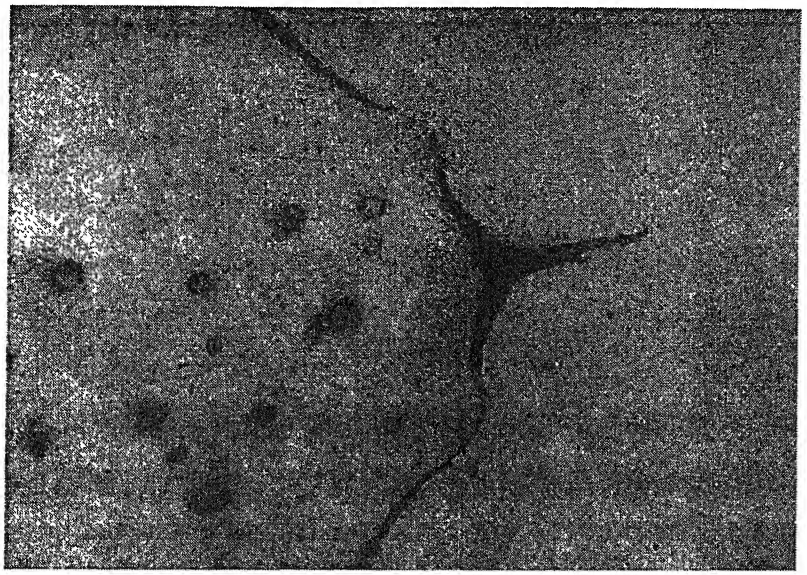

Fig.3.5. The microstructure of Al-3.6wt% Cu alloy, annealed at 615°C in the α+liquid field for 12 h and then down-quenched to 580°C in the α phase field and held for 90 s. Magnification 500X.

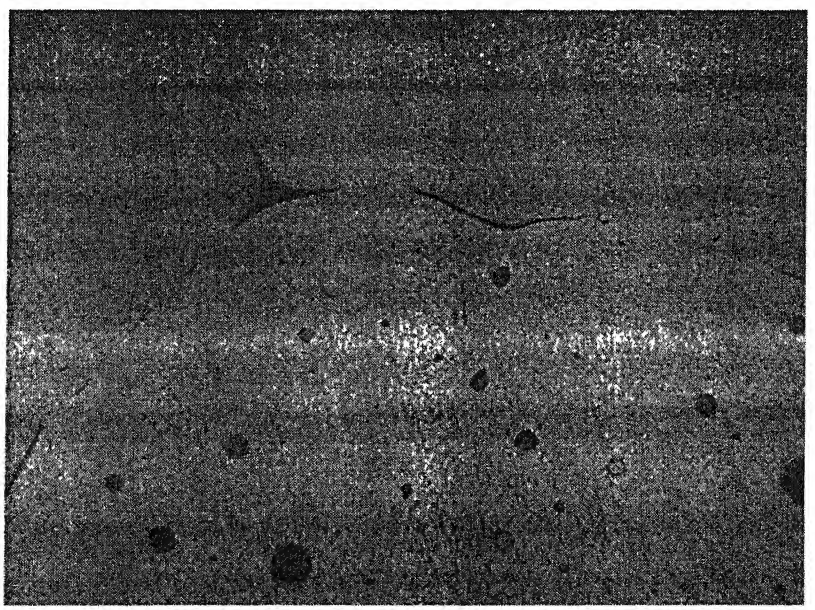

Fig.3.6. The microstructure of Al-3.6wt% Cu alloy, annealed at 615°C in the α+liquid field for 12 h and then down-quenched to 580°C in the α phase field and held for 3min. Magnification 200X.

Fig 3.7. is the microstructure showing LFM that has occurred when the sample is down quenched to 580°C and held for 5 min. It has been observed that the migration rate of the liquid film in the center of the curved boundary has decreased whereas it keeps growing at the ends resulting into a flat boundary. The reason for such a behavior could be retained from the presence of solute source at the triple point, which makes the distance smaller at the end of the film than at the center.

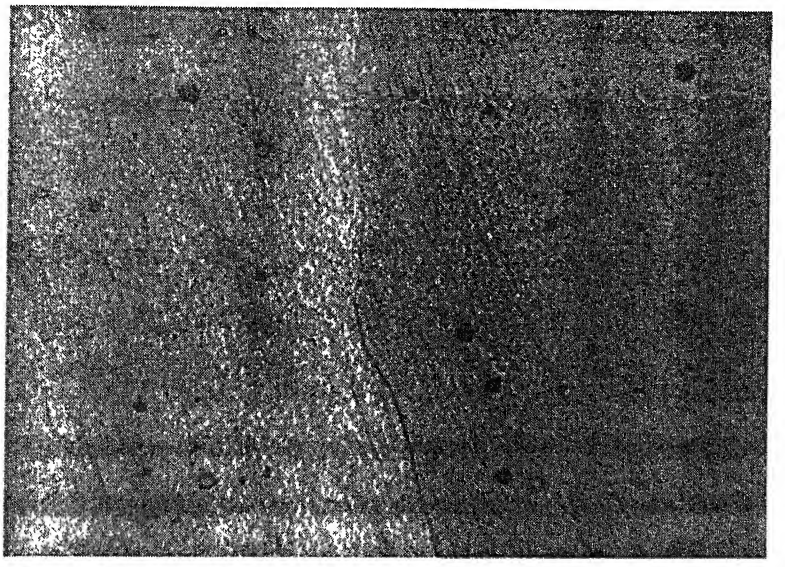

Fig.3.7. The microstructure of Al-3.6wt% Cu alloy, annealed at 615°C in the α+liquid field for 12 h and then down-quenched to 580°C in the α phase field and held for 5min. Magnification 200X.

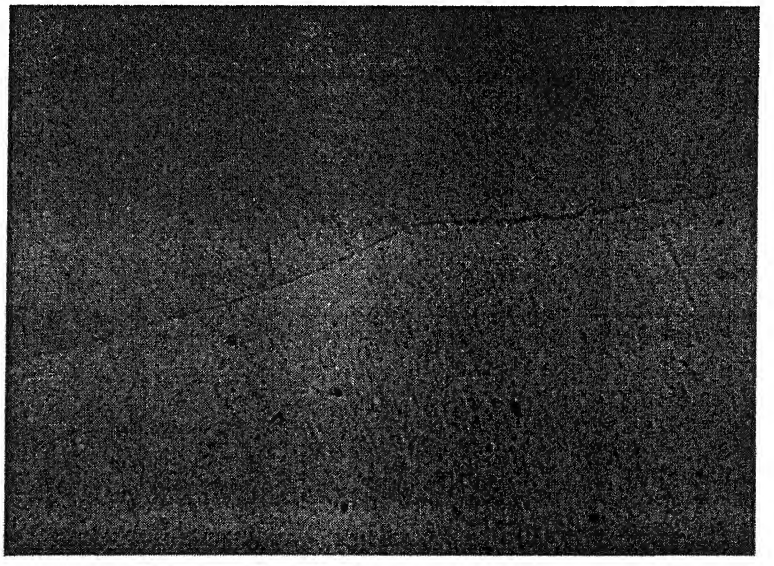

Fig.3.8. The microstructure of Al-3.6wt% Cu alloy, annealed at 615°C in the α+liquid field for 12 h and then down-quenched to 580°C in the α phase field and held for 10min. Magnification 200X.

From Fig.3.8 it can be said that after holding 10 min. at the 580°C, all liquid has exhausted forming grain boundaries. The newly formed grain boundaries are clearly visible in the above microstructure.

Fig.3.9 is a microstructure showing LFM that has occurred when an Al-3.6wt% Cu alloy sample is up-quenched to 647°C in the alpha + liquid field from 615°C and held for 5 s. The liquid films are observed to be bulging out with small radii of curvature indicating the start of migration. Second phase distributed as globules in the microstructure is the liquid formed during annealing.

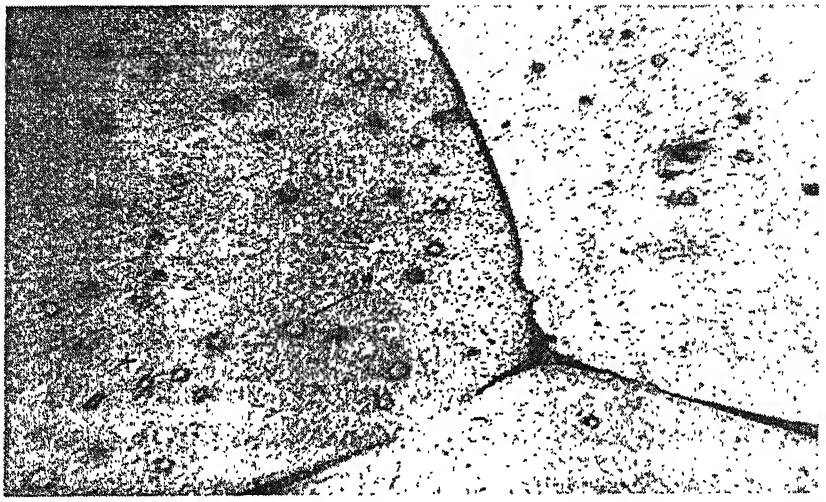

Fig.3.9. The microstructure of Al-3.6wt% Cu alloy, annealed at 615°C in the α+liquid field for 12 h and then up-quenched to 637°C in the α+liquid field and held for 5 s. Magnification 200X.

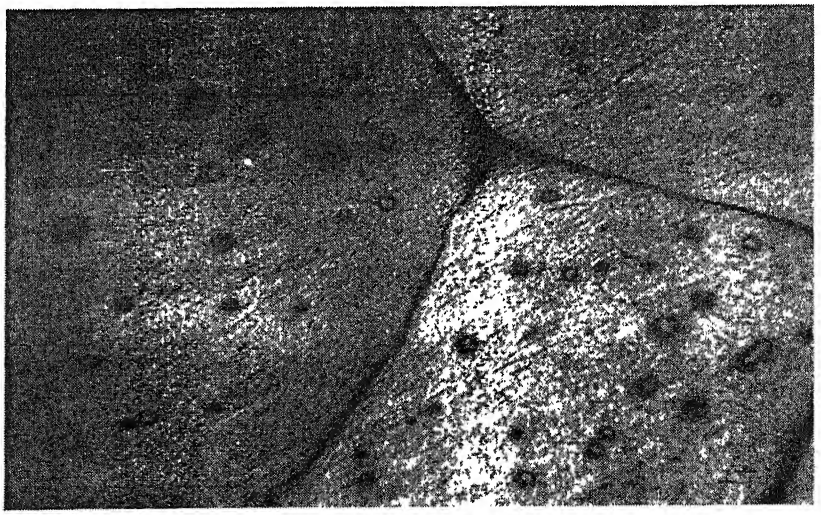

Fig.3.10. The microstructure of Al-3.6wt% Cu alloy, annealed at 615°C in the α+liquid field for 12 h and then up-quenched to 637°C in the α+liquid field and held for 10 s. Magnification 200X.

Fig.3.10 is a microstructure showing LFM that has occurred when the alloy sample is up-quenched to 637°C and held for 10 s. The migration distance has increased with time. The regions swept by the liquid film are expected to be depleted of solute. Since the sample is up-quenched the amount of liquid at the triple points, prior grain boundaries and within the grains increased as the time of transformation increases.

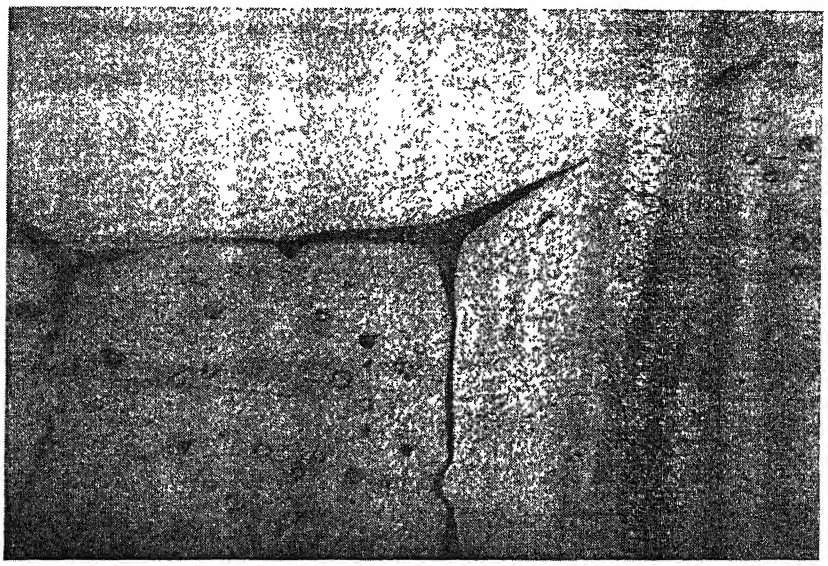

Fig.3.11. The microstructure of Al-3.6wt% Cu alloy, annealed at 615°C in the α+liquid field for 12 h and then up-quenched to 637°C in the α+liquid field and held for 20 s. Magnification 200X.

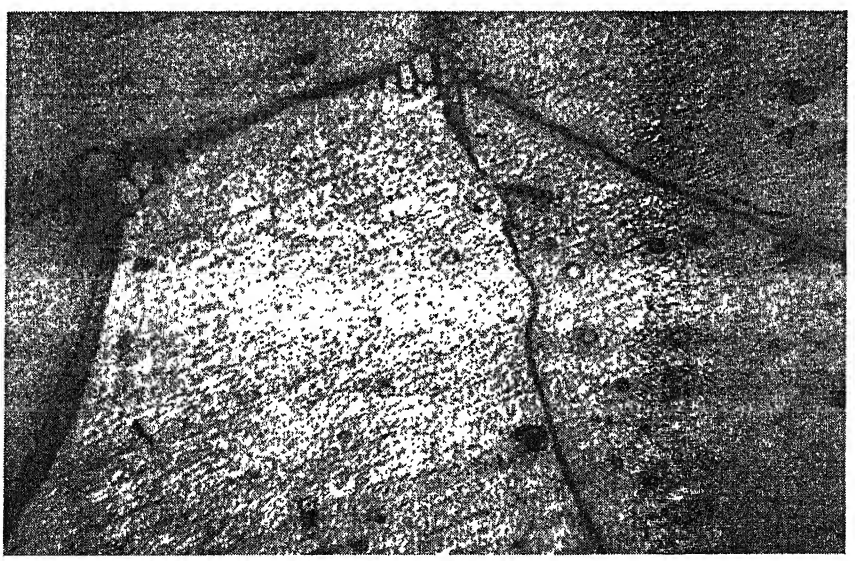

Fig.3.12. The microstructure of Al-3.6wt% Cu alloy, annealed at 615°C in the α+liquid field for 12 h and then up-quenched to 637°C in the α+liquid field and held for 40 s. Magnification 200X.

Fig.3.11 is a microstructure showing LFM that has occurred when the alloy sample is up-quenched to 637°C and held for 20s. The solute from the depleted matrix formed behind the moving liquid film is expected to increase the volume fraction of the liquid. The thickness of the migrating liquid film has been observed to increase.

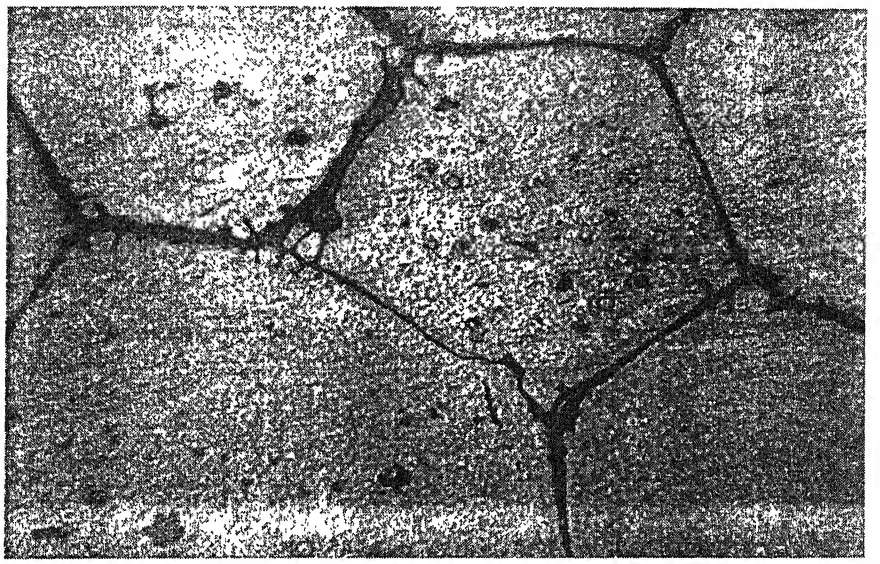

Fig.3.13. The microstructure of Al-3.6wt% Cu alloy, annealed at 615°C in the α+liquid field for 12 h and then up-quenched to 637°C in the α+liquid field and held for 90 s. Magnification 200X.

Fig.3.12 is a microstructure showing LFM that has occurred when the alloy sample is up quenched to 637°C and held for 40 s. The migration distance and radius of curvature is observed to increase with time. The amount of liquid at triple points has increased. The liquid film has not become flat, as was the case during down-quenching experiments.

Fig.3.13 is a microstructure showing LFM that has occurred when the alloy sample is up quenched to 637°C and held for 90 s. The rate of migration was observed to decrease as the time of transformation increased. This is due to the decrease in driving force as the amount of liquid phase grows with time resulting in the loss of solute from the matrix in front of the migrating liquid film.

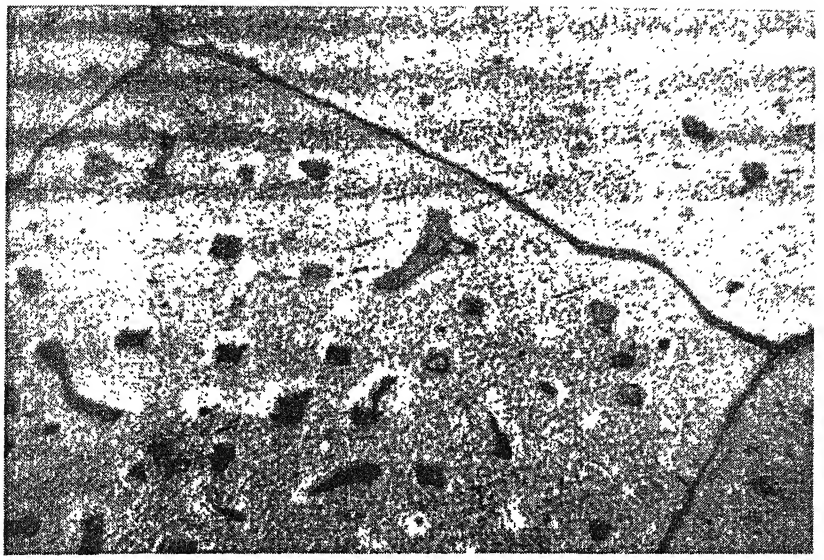

Fig.3.14. The microstructure of Al-3.6wt% Cu alloy, annealed at 615°C in the α+liquid field for 12 h and then up-quenched to 637°C in the α+liquid field and held for 3 min. Magnification 200X.

Fig.3.14 is a microstructure showing LFM that has occurred when the alloy sample is up quenched to 637°C and held for 3 min. As seen in the microstructure, a thick liquid film approximately 5 μm has been able to migrate. High diffusivities of solute as well as the solvent atoms at the higher temperatures appeared to be the reasons for this.

Fig.3.15 is a microstructure showing LFM that has occurred when the alloy sample is up quenched to 637°C and held for 10 min. The radius of curvature of migrating boundary has increased with time.

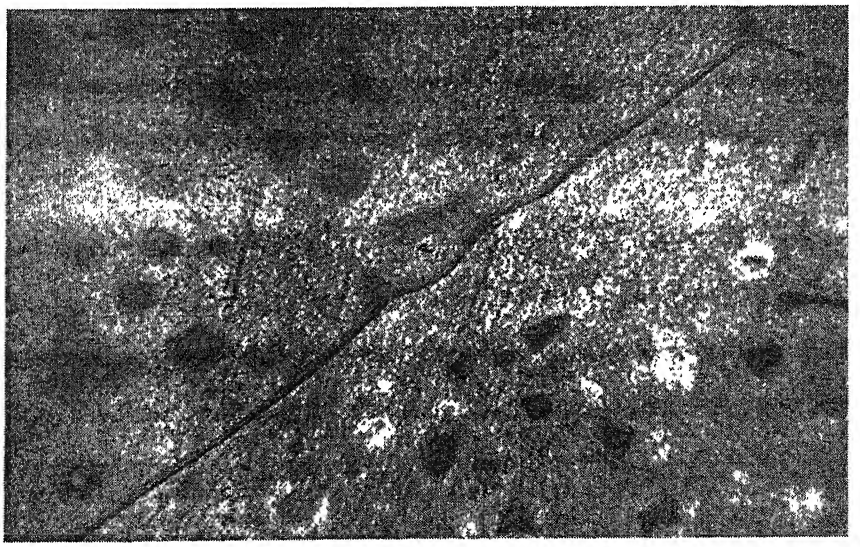

Fig.3.15. The microstructure of Al-3.6wt% Cu alloy, annealed at 615°C in the α+liquid field for 12 h and then up-quenched to 637°C in the α+liquid field and held for 10 min. Magnification 200X.

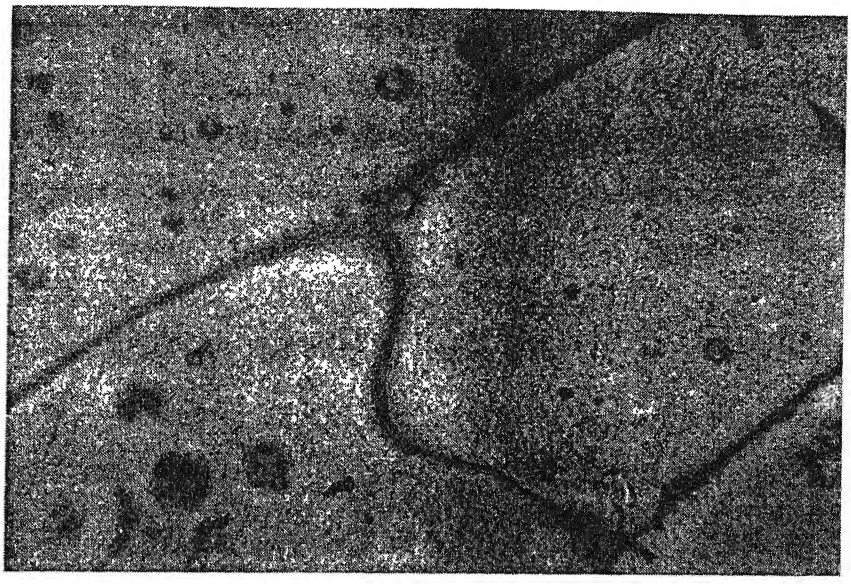

Fig.3.16. The microstructure of Al-3.6wt% Cu alloy, annealed at 615°C in the α+liquid field for 12 h and then up-quenched to 637°C in the α+liquid field and held for 30 min. Magnification 200X.

Fig.3.16 is a microstructure showing LFM that has occurred when the alloy sample is up quenched to 637°C and held for 30 min. Migration of the film even after 30 min. has not stopped as there is no paucity of solute from the source. The migration velocity is found to decrease as the time of transformation increased, and this is due to a decrease in the driving force that has resulted due to a decrease in concentration gradient between the grain in front of the migrating film and the area swept by the migrating film.

3.2 liquid film migration rates

The migration distances were measured with the help of a reticule as a function of time during LFM at 500, 520, 540, 560, 580, 590, 627, 637 and 647°C respectively. The migration distances for the given time and temperature were taken to be the average of 40 measurements of the maximum migration distance of a boundary or liquid film from its initial position to its final position. Only the migration of those boundaries and liquid films, which had migrated, was considered in the averaging.

The average migration distance was plotted against the time of annealing. The plot shows a parabolic growth rate, which is shown in Fig.3.17. The LFM data are shown in tables 3.1 and 3.2 for down-quench and up-quench treatments, respectively. The average migration distance at a particular temperature increases monotonically with annealing time with the rate of migration decreasing monotonically. This behavior was observed at all temperatures. It is presumed that the decrease in migration rate is associated with a decrease in the driving force resulting from the dissolution of the spheres of liquid or θ phase for the down-quenching experiments or their growth for the up-quenching experiments. For the down-quench experiments the dissolution of the spheres cause the gradual increase in the Cu content of the α grains and subsequent loss of driving force for alloying type DIGM or LFM. The opposite is true for the up-quench experiments, for which the growth of liquid spheres and the subsequent decrease in the Cu content of the α phase results in a loss of driving force for the dealloying type of LFM. The rate of migration can be determined from the tangent to the curves shown in Figs.3.17 and 3.18. It appears to be high initially. However, as the time of treatment is increased, the rate of migration decreased.

The migration distance was plotted against the time of annealing on a log-log scale, Figs.3.19 and 3.20. It shows a linear behavior. The data can be represented by the equation

$$x = kt^n \qquad (10)$$

where x is the migration distance during LFM, and t is the time of annealing. The slopes of the lines were calculated at each temperature. The corresponding n values ranged from 0.2 to 0.25 in this system. The result is consistent with those reported by Kuo and Fourenlle [19] in their work on this system.

The growth rate can be calculated by differentiating equation (10) and we get

$$v = \frac{dx}{dt} = n.k.t^{n-1} = \frac{nx}{t}$$

The growth rate was calculated from the above equation at all temperatures and the values are shown in tables 3.3 and 3.4. The growth rate was plotted against the time of treatment, Figs.3.21 and 3.22. It is clear from Fig.3.21 and table 3.4 that at any particular temperature the growth rate decrease with an increase in the time of annealing. This can be explained from the decreasing driving force with the increase in the time of treatment by the change in solute concentration in α grains due dissolution or growth of the θ phase. It can also be observed from Fig.3.21 and table 3.4 that at any given annealing time the growth rate for LFM increase with increasing temperature. As the temperature increases the driving force increases which results in the increase in the migration rate. However, this increase in growth rate with temperature at any time has been low in this system due to the second phase effect within the grains. There is a strong dependence of temperature on LFM. It has been explained by Yoon [19] that if the temperature is very high there is a possibility that the frontal diffusion zone given by D_v/v can increase to such a large value that coherency cannot be maintained and hence the driving force becomes zero and the migration of the interface stops. This phenomenon was not observed in this investigation. But, at higher annealing times i.e 30 to 60 min. at all temperatures, all grain boundaries were straight and all the migrated boundaries were seemed to be reaching equilibrium configuration. This can be explained by the fact that at higher annealing times there is enough time for volume diffusion to occur and the system tends towards its equilibrium state at that particular temperature. The concentration gradient set up behind the migrating grain boundaries will gradually decrease and the net flux of atom will accordingly decrease resulting ultimately into homogeneous solid and liquid solutions. The additional energy associated with the curved boundaries will be dissipated for the boundary migration. The final microstructure will show straight grain boundaries as these are of equilibrium configuration to be associated with the least energy of the system.

Time, s	Migration distance, x in μm for LFM by down-quenching from α+liquid region to single phase region					
	500°C	520°C	540°C	560°C	580°C	590°C
5	11.2	12.45	13.42	14.63	15.6	17.29
10	13.1	14.48	15.8	16.73	17.97	19.34
20	14.98	16.99	18.32	19.54	21.1	22.92
40	17.56	19.41	21.01	22.59	23.43	26.91
90	20.01	22.18	23.97	25.93	27.77	33.35
180	22.69	25.1	27.36	29.93	32.17	39.53
300	25.17	27.61	31.19	33.52	35.82	45.35
600	28.92	32.24	34.59	37.58	40.37	52.43

Table 3.1. Migration of liquid films for LFM at different temperatures of down-quenching experiments.

Time, s	Migration distance, x in μm at different temperatures for LFM		
	627°C	637°C	647°C
5	12.61	16.19	17.9
10	15.25	18.34	20.4
20	17.49	21.92	23.78
40	21.47	25.91	27.99
90	25.26	32.35	35.89
180	30.16	38.43	43.59
300	34.62	44.35	
600	40.85	51.67	

Table 3.2. Migration distance for LFM at different up-quench temperatures.

Time, s	Growth rate, μm s^{-1} for LFM measured at different temperatures for down-quenching treatments.					
	500°C	520°C	540°C	560°C	580°C	590°C
5	0.43	0.50	0.54	0.59	0.62	0.86
10	0.25	0.29	0.32	0.34	0.36	048
20	0.14	0.17	0.18	0.20	0.21	0.28
40	0.08	0.09	0.11	0.113	0.117	0.17
90	0.04	0.05	0.053	0.058	0.062	0.09
180	0.02	0.03	0.031	0.033	0.035	0.05
300	0.01	0.018	0.021	0.022	0.024	0.04
600	0.009	0.011	0.012	0.013	0.014	0.02

Table 3.3. Growth rate as a function of time during LFM for down-quenching experiments.

Time, s	Growth rate, μm s^{-1} for LFM measured at different temperatures for up-quenching		
	627°C	637°C	647°C
5	0.6305	0.8095	0.895
10	0.3813	0.4585	0.51
20	0.2186	0.274	0.2973
40	0.1342	0.1619	0.175
90	0.0702	0.0897	0.0997
180	0.0419	0.0534	0.0605
300	0.0289	0.037	
600	0.017	0.0215	

Table 3.4. Growth rate as a function of time for LFM at different up-quenching experiments.

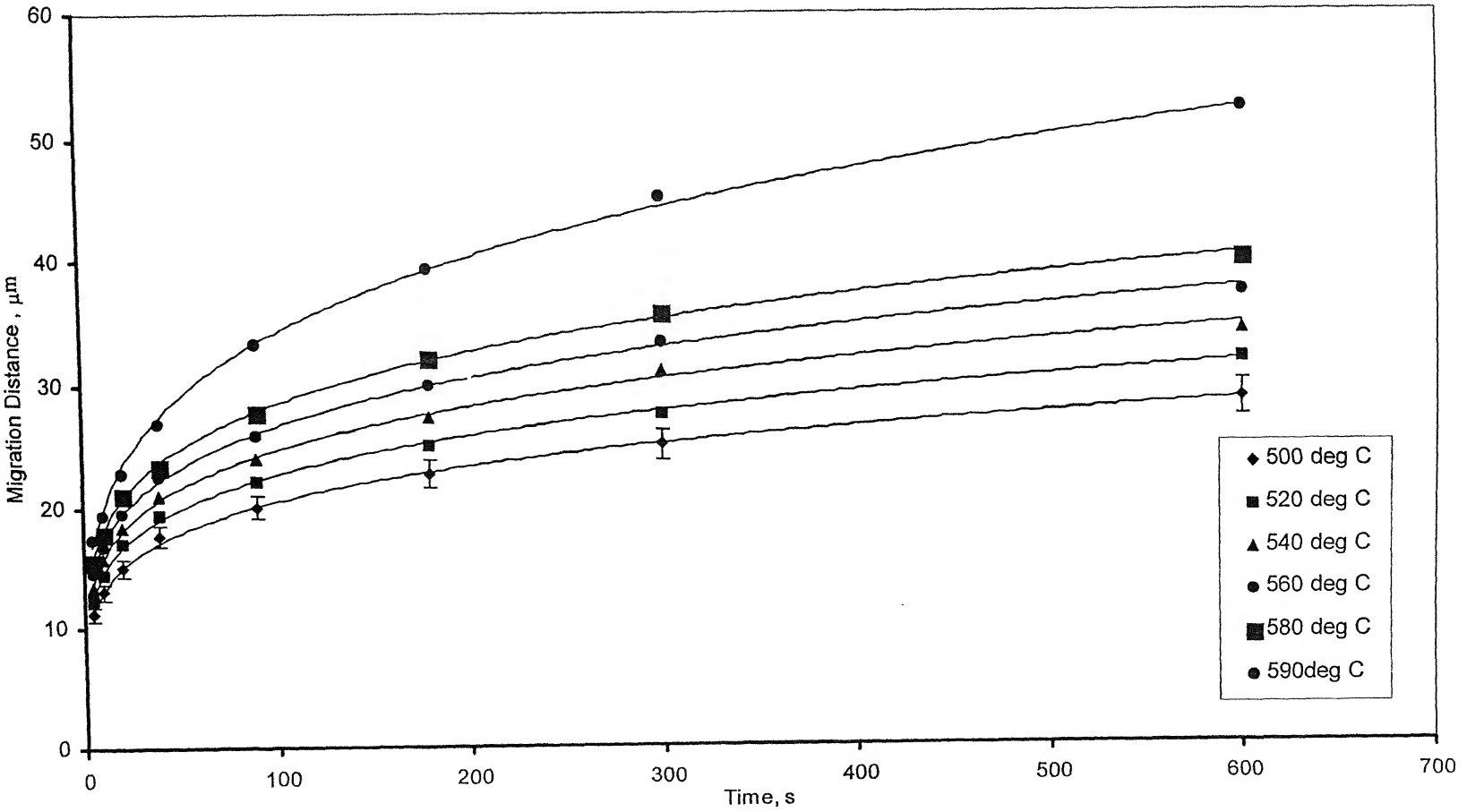

Fig 3.17. Plot of Migration Distance as a function of Time for LFM at different temperatures of down-quenching experiments.

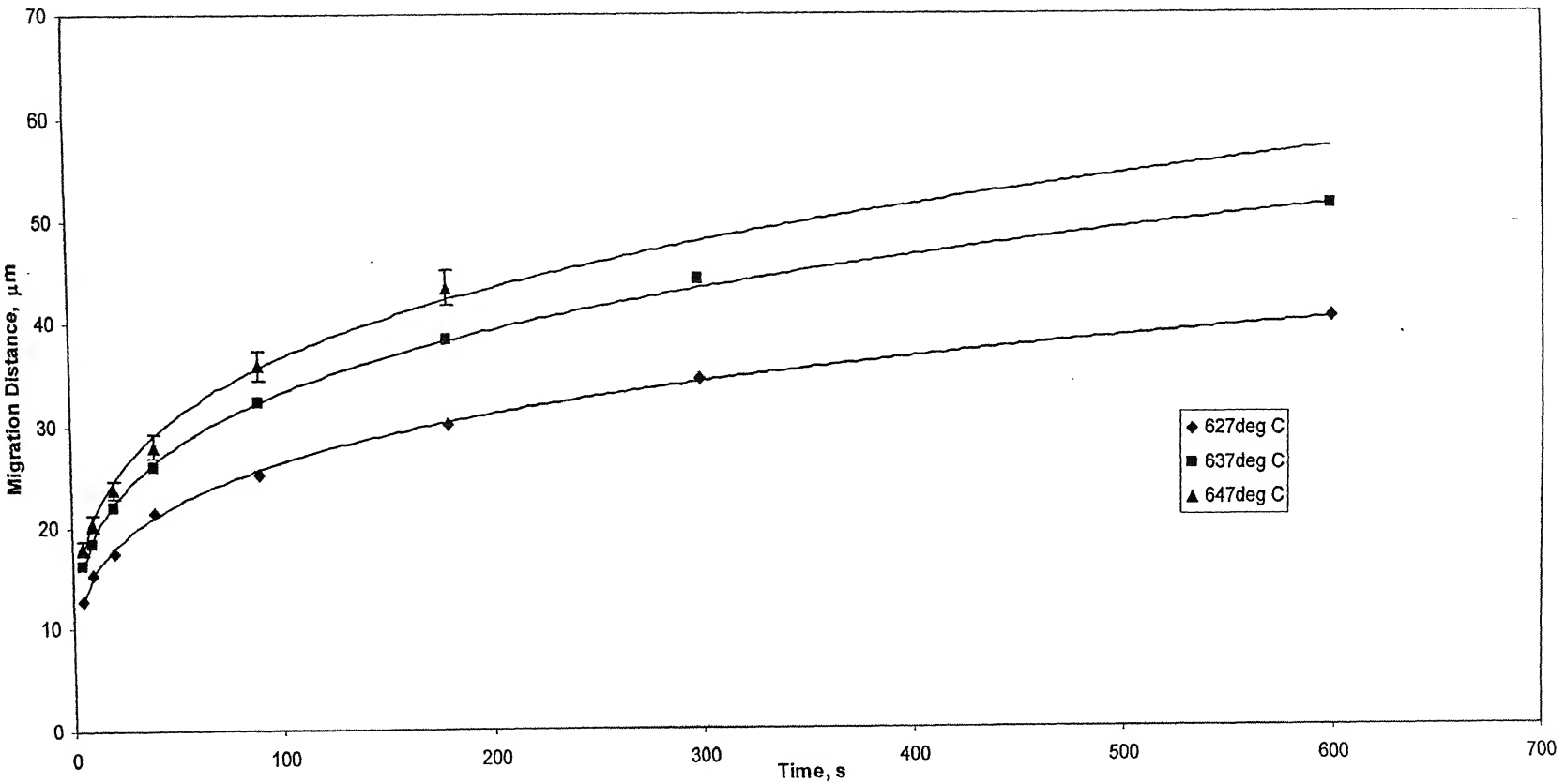

Fig 3.18. Plot of Migration Distance as a function of Time for LFM at differnet temperatures of up-quenching experiments.

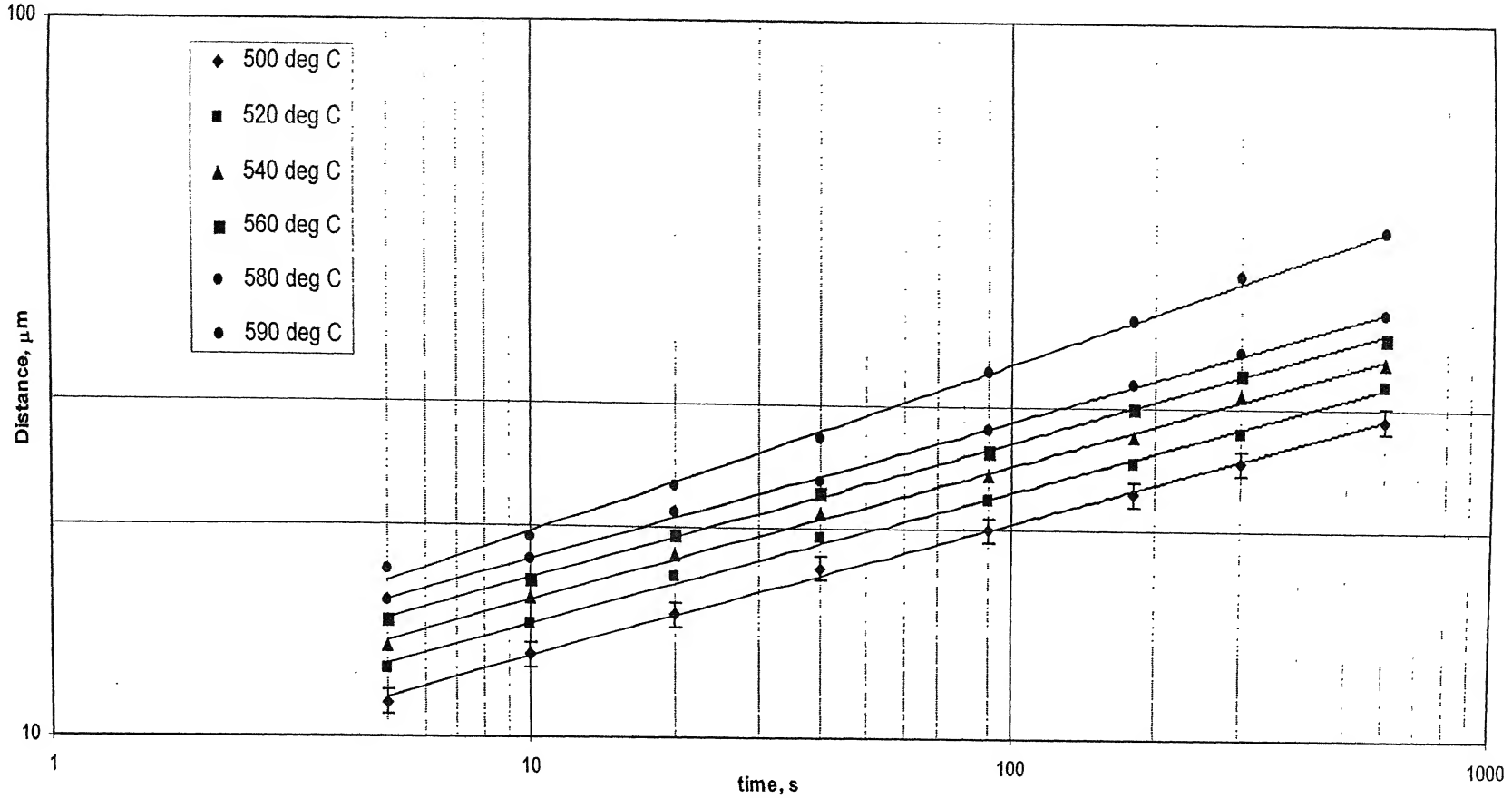

Fig 3.19. log distance vs log time plot at different temperatures of down-quenching experiments for LFM

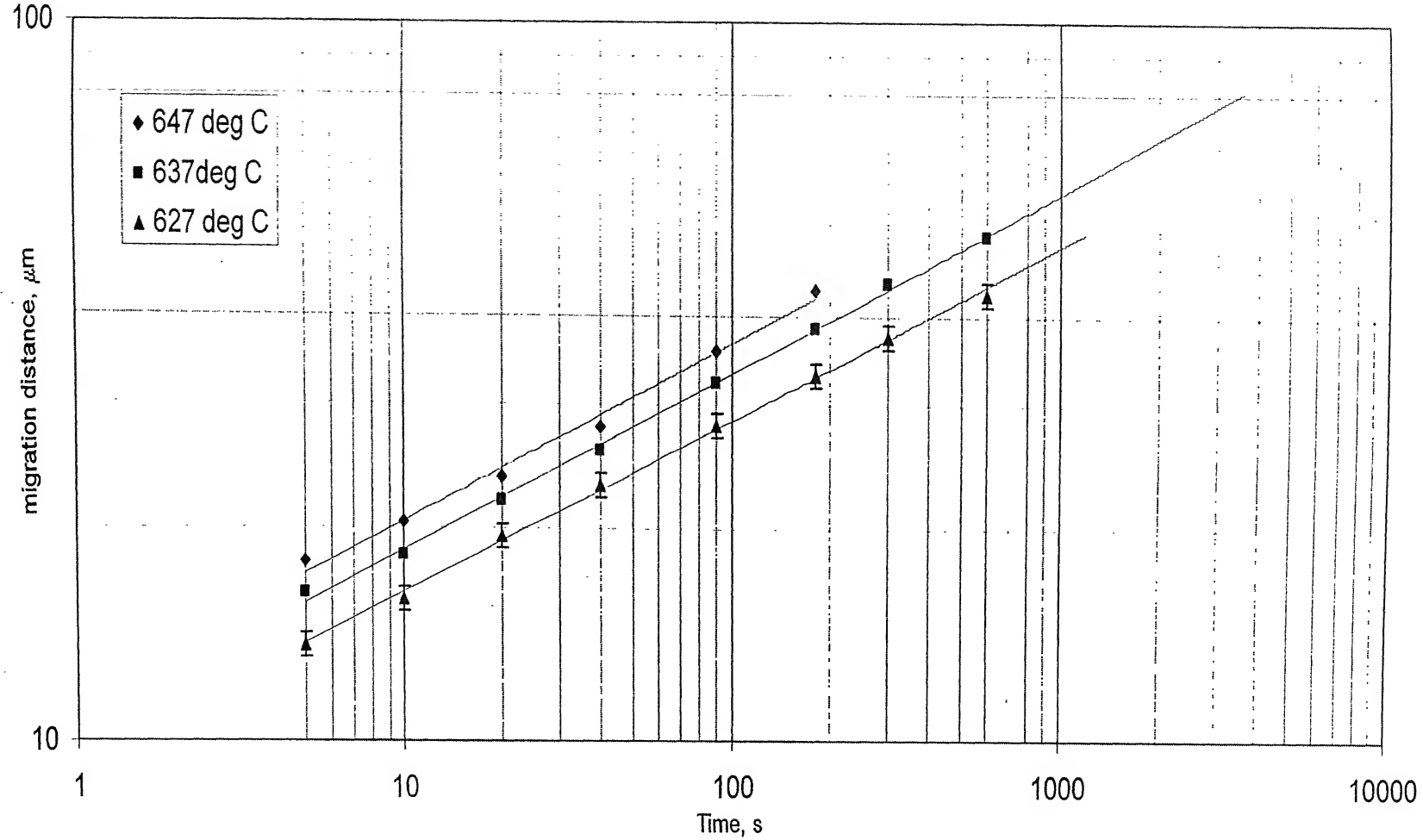

Fig 3.20. log distance vs log time plot at different temperatues of up-quenching experiments for LFM

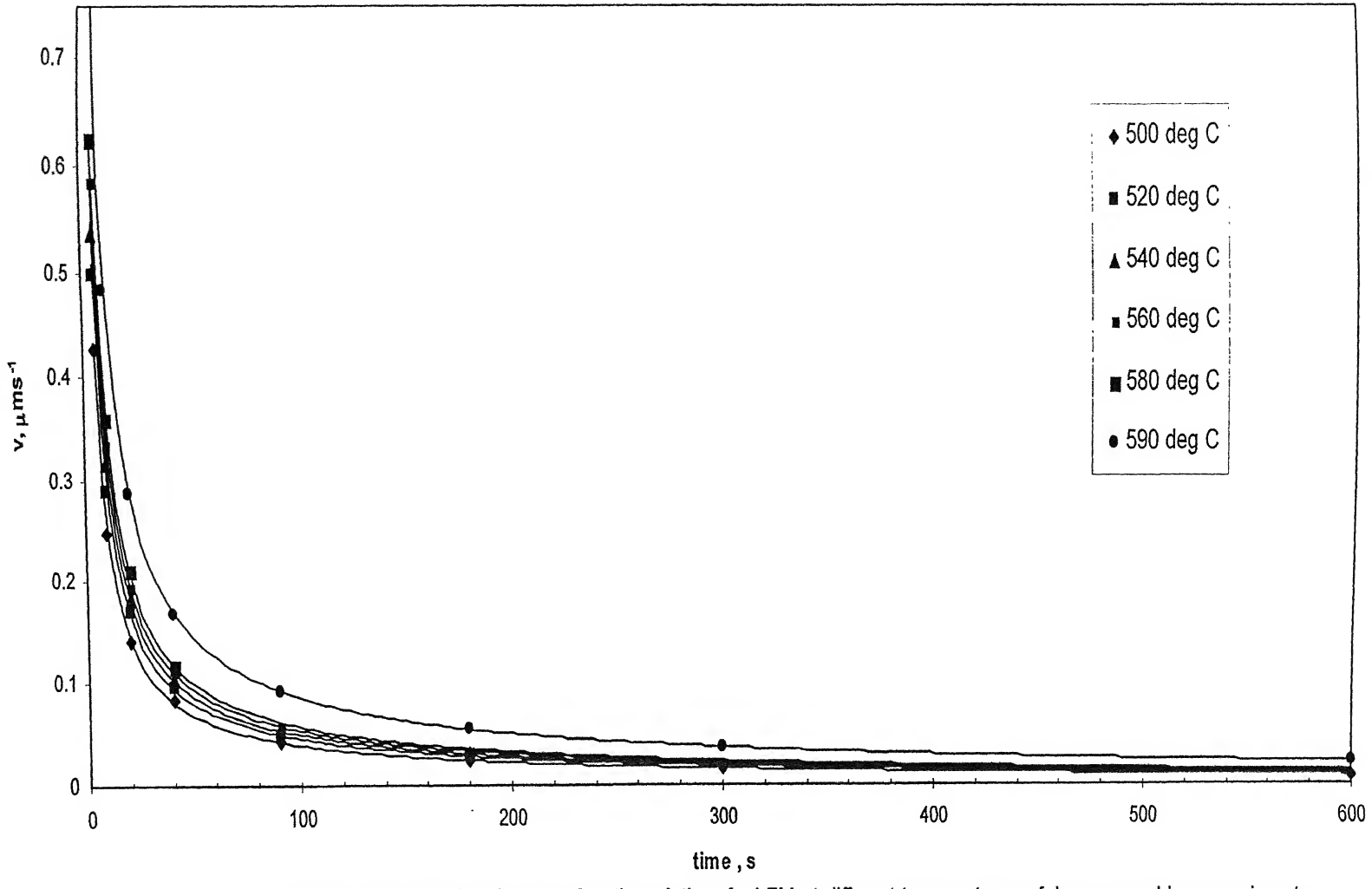

Fig 3.21. Rate of migration as a function of time for LFM at differnet temperatures of down-quenching experiments.

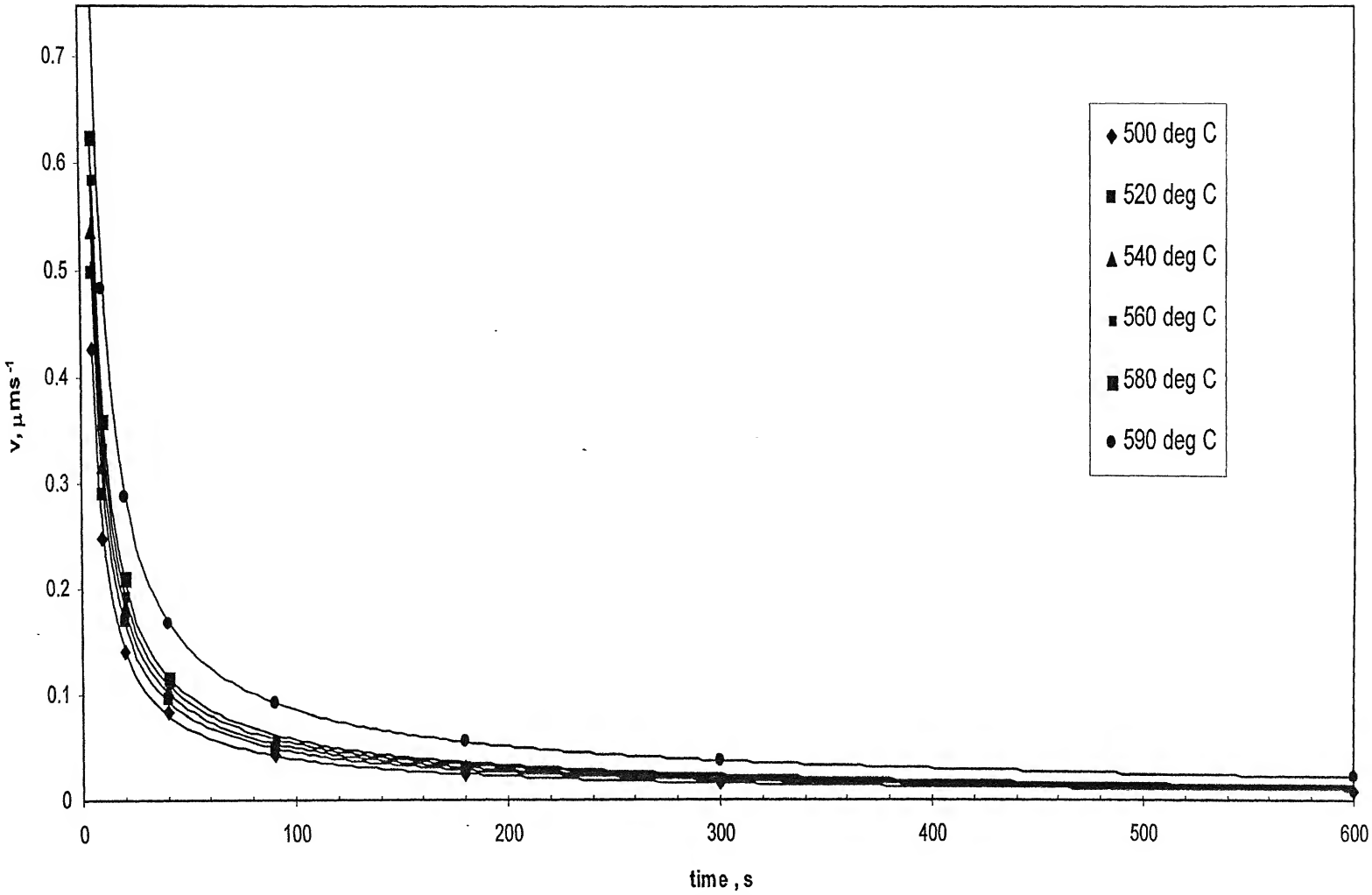

Fig 3.21. Rate of migration as a function of time for LFM at differnet temperatures of down-quenching experiments.

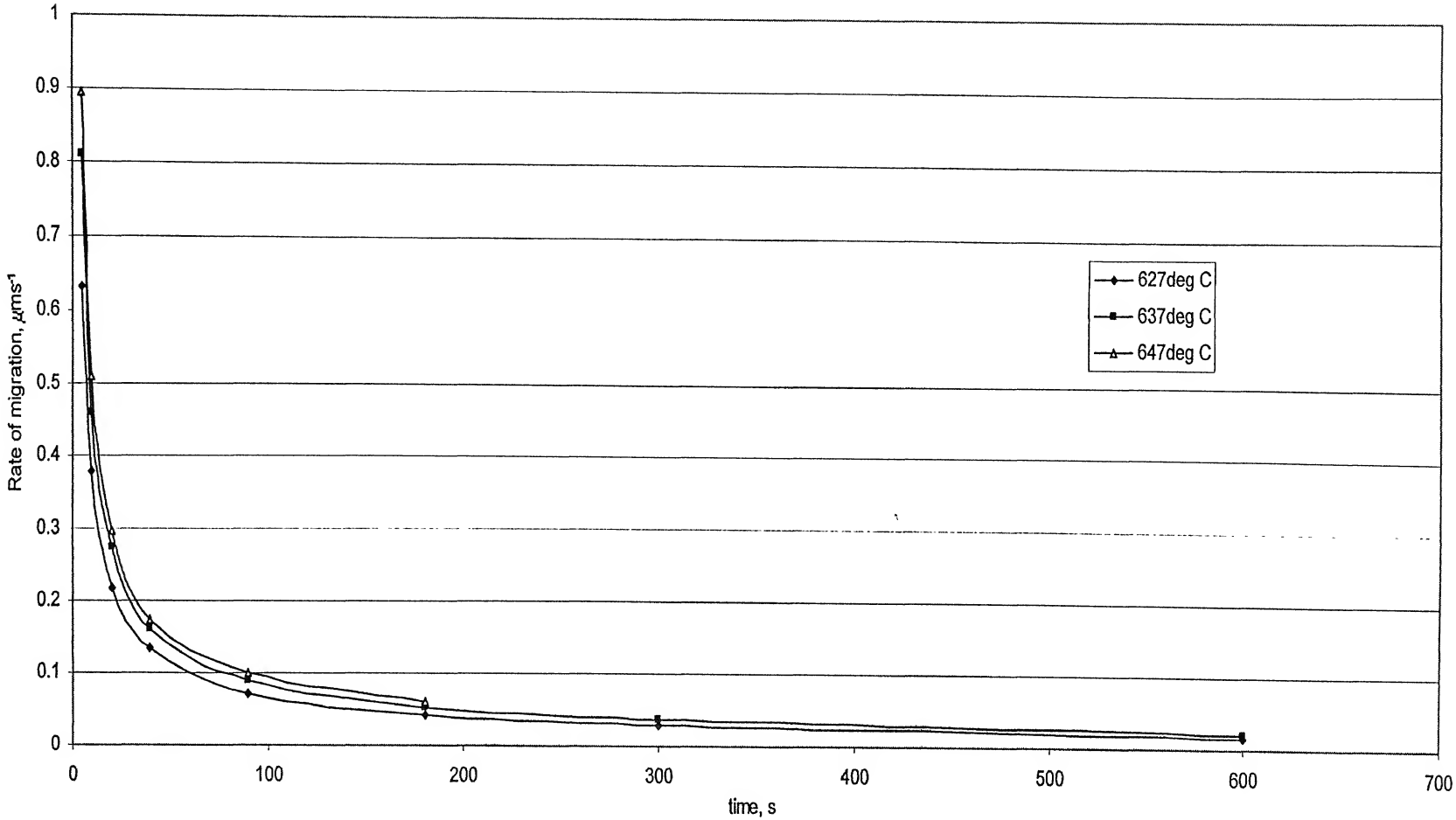

Fig 3.22. Rate of migration as a function of time for LFM at differnet tempetatures of up-quenching experiments.

3.3 Discussion

There has been considerable experimental evidence that the coherency strain developed in the grain being consumed during LFM or DIGM due to volume diffusion of the solute into the receding grain being the driving force for the above mentioned reactions. In order to evaluate the coherency strain as the driving force for liquid film migration in the present study values of the volume diffusion penetration distance ahead of the migrating liquid film as well as the magnitude of the coherency strain itself were calculated and compared with the free energy differences associated with the liquid film migration. Table 3.5 shows values of the volume diffusion penetration distance D_v/v ahead of migrating liquid film for various annealing temperatures.

Table 3.5. Volume diffusion penetration distance (D_v/v) in advance of migrating liquid films after 5 s.

Reaction	Temp. (°C)	D_v , (m^2s^{-1})	V, ($\mu m\ s^{-1}$)	D_v/v, (μm)
LFM	500	4.21×10^{-14}	0.43	0.09
LFM	520	7.19×10^{-14}	0.5	0.14
LFM	540	1.19×10^{-13}	0.54	0.22
LFM	560	1.94×10^{-13}	0.59	0.33
LFM	580	3.07×10^{-13}	0.62	0.49
LFM	590	3.83×10^{-13}	0.75	0.51
LFM	627	8.36×10^{-13}	0.63	1.32
LFM	637	1.02×10^{-12}	0.81	1.35
LFM	647	1.24×10^{-12}	0.9	1.38

The D_v values were calculated from the following equation, taken from the reference 20]

$$D_v = 0.654\times10^{-4}\exp\left(\frac{-136000 Jmol^{-1}}{RT}\right)m^2s^{-1} \qquad (10)$$

The calculated D_v/v values in table 3.5 are just at the beginning of the migration i.e. after 5 s. As the velocity of migration decreases monotonically with annealing time, the solute penetration will be much higher at longer times. As can be seen the penetration distances are on the order of 0.1 to 1μm, and, thus, considerable

penetration of Cu ahead of the migrating films is expected. For the fastest migration rate at the highest temperature (647°C), the penetration distance is about 3400 lattice parameters of Al lattice, and for the slowest migration rate at the lowest temperature (500°C), the penetration distance about 220 lattice parameters of Al lattice after 5 s. Thus, there has been sufficient penetration by Cu at all temperatures to insure development of a coherently strained layer.

According to the coherency strain theory [11] the strain energy per unit volume developed in the surface of a grain into, or out of, which solute atoms have diffused is given by equation,

$$\Delta G_{coh} = \frac{E\eta^2 V_m (X_{Cu}^{l} - X_{Cu}^{o})^2}{1-\nu}$$

Table 3.6 shows values of ΔG_ε calculated for the up and down-quench LFM experiments. According to Sutton [21] $E_{<100>}$ and $E_{<111>}$ have values of 43.1 and 55.5 GPa respectively, and $\nu_{<100>}$ and $\nu_{<111>}$ have values of 0.319 and 0.345 at 500°C for Al. The misfit parameter is given by $\eta = \frac{1}{a}\left(\frac{da}{dX_{Cu}}\right)$, where a is the lattice parameter. The data given by Pearson [22] were used, and $\frac{da}{dX_{Cu}}$ was calculated from the composition dependant lattice parameter data given by Murray [13]. The values of X_{Cu}^{α} and X_{Cu}^{o} were taken from equilibrium phase diagram. The resulting values of $\Delta G_\varepsilon^{<100>}$ and $\Delta G_\varepsilon^{<111>}$ are given in table 3.6 and represent the minimum and maximum values of ΔG_ε, respectively. These define the limits to the range of ΔG_ε values possible. In addition to that, values of minimum radius of curvature (r_{min}) of liquid film supportable by the coherency strain energy were calculated from the $\Delta G_\varepsilon^{<111>}$ values using equation

$$\Delta G_\varepsilon^{<111>} = \frac{\gamma}{r_{min}} \qquad (11)$$

where γ is the surface energy per unit area of the α/liquid interface. Here the value of $\gamma = 0.1634$ J m^{-2} at 821 K given by Gunduz and Hunt [23] was used.

Temp, °C	X^{l}_{Cu}	X^{o}_{Cu}	$\Delta G_{\varepsilon}^{<100>}$, J mol^{-1}	$\Delta G_{\varepsilon}^{<111>}$, J mol^{-1}	ΔG, Eq. (9) J mol^{-1}	ΔG, Eq. (2) J mol^{-1}	r_{min}, μm	r, μm (experimental)	ΔG^{γ}, J mol^{-1} (experimental)
647	0.00159	0.00728	0.486	0.657	-17.0		2.2	12.08	0.2597
637	0.00326	0.00728	0.243	0.324	-8.39		4.5	11.04	0.2851
627	0.00461	0.00728	0.108	0.144	-3.67		10.0	9.7	0.3255
615	annealing temperature				0				
590	0.01234	0.00728	0.387	0.522	-12.62		2.8	12.83	0.2489
580	0.0157	0.00728	1.0728	1.4364	-34.53	-37.8	1.02	18.4	0.1741
560	0.0157	0.00728	1.0728	1.4364	-33.72	-36.9	1.03	17.44	0.1848
540	0.0157	0.00728	1.0728	1.4364	-32.91	-36.0	1.04	16.38	0.198
520	0.0157	0.00728	1.0728	1.4364	-32.10	-35.1	1.05	15.53	0.2101
500	0.0157	0.00728	1.0728	1.4364	-31.28	-33.3	1.06	14.7	0.2233

Table 3.6. Coherency strain energies and chemical free energy changes at different temperatures.

Chemical free energy change for the migration of liquid film was calculated from two different equations, (2) and (9) sited earlier and are shown in table 3.6 for comparison. As can be seen from table 3.6, the coherency strain energies are much smaller in comparison with the chemical free energy change values. The estimated radii [r] are greater than (r_{min}) calculated from the coherency strain energy. Thus it appears that the coherency strain energy cannot account for the observed curvatures of the liquid films in the present study and is clearly insufficient to drive the migration.

The equation to determine the Copper concentration difference, ΔX_B across the planar liquid film, which can be determined by elastic constants, atomic misfits, equilibrium solubilities and solution thermodynamic properties of the liquid and solid phases as given by Brechet and Purdy [24].

$$\Delta X_B = \left[\frac{Y\eta^2 RTV_m}{2X_B^S Y\eta^2 V_m + RT} \left[X_B^o - \left(X_B^L - \Delta X_B \right) k \right]^2 + 2\gamma K V_m \right] \frac{\left(1 - \frac{X_B^S}{k} \right)}{RT(1-k)} \qquad (12)$$

where Y is the appropriate orientation dependent modulus of elasticity, η is a linear expansion coefficient due to solute addition. γ is the specific solid-liquid interfacial free energy, K is the interfacial curvature, V_m is the molar volume.

The modulus of elasticity values were taken from Sutton [21] as 43.1 and 55.5 GPa for <100> and <111> directions respectively. The interfacial free energy is given by, $\Delta G^{\gamma} = \frac{2\gamma V_m}{r}$, where γ is the specific solid-liquid interfacial energy and, r is the radius of curved migrating grain boundary, measured from the microstructures taken from optical microscope at 200X magnification for one particular time of treatment. X_B^S, X_B^L and X_B^o are solute concentration of the region left behind the migrating grain boundary, composition of the liquid film/dealloyed zone interface and composition of the grain well away from migrating liquid film respectively. These composition values were obtained from the equilibrium phase diagram. After solving the equation (12), the value obtained for the difference in solute concentration across the migrating planar liquid film at different temperatures of up-quenching and down-quenching treatments are shown in table 3.7. The solute concentration across migrating liquid film vs. migration distance profile was shown in Fig.3.23 for up-quenching and for down-quenching in Fig 3.24.

From table 3.7 it can be concluded that the copper concentration difference across the film decreases with an increase in temperature of reaction. The $\overline{X}_B^S$ is given as $(X_B^L - \Delta X_B)k$. It approaches X_B^S as the temperature of the reaction is increased.

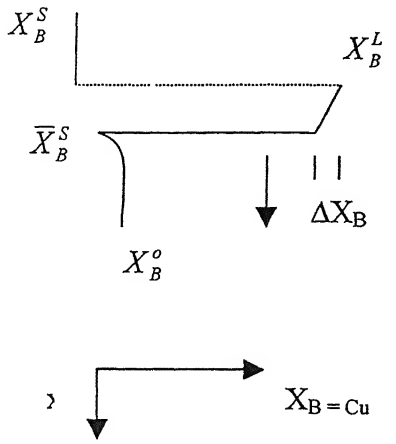

Fig.3.23. Copper concentration profile across the migrating liquid film for up-quenching experiments.

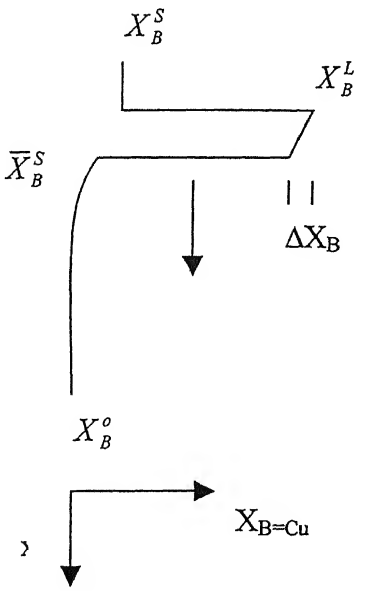

Fig.3.24. Copper concentration profile across the migrating liquid film for down-quenching experiments.

Table 3.7. Cu concentration difference, ΔX_B, at different down and up-quenching experiments.

Temp. °C	X_B^o	X_B^S	X_B^L	k	ΔX_B
647	0.00728	0.00461	0.0382	0.1207	0.544×10^{-4}
637	0.00728	0.00326	0.0296	0.11	0.570×10^{-4}
627	0.00728	0.00159	0.0191	0.0833	0.613×10^{-4}
590	0.00728	0.01234	0.0954	0.1293	0.597×10^{-4}
580	0.00728	0.0157	0.12142	0.1293	0.8835×10^{-4}
560	0.00728	0.0157	0.12142	0.1293	0.91×10^{-4}
540	0.00728	0.0157	0.12142	0.1293	0.948×10^{-4}
520	0.00728	0.0157	0.12142	0.1293	1.006×10^{-4}
500	0.00728	0.0157	0.12142	0.1293	1.052×10^{-4}

Table 3.8. Diffusion Coefficient of Cu in the liquid film at different down and up-quenching experiments.

Temp, °C	Time, s	Thickness of the liquid film (δ), μm	Growth distance(x), μm	Velocity (v), μm s^{-1}	Diffusion coefficient of Cu in the liquid film,(D_L), m^2 s^{-1}
500	5	1.91	7.27	0.2908	0.783×10^{-9}
520	5	1.82	10	0.4	1.074×10^{-9}
540	5	1.5	14.5	0.58	1.3603×10^{-9}
560	5	1.36	17.4	0.69	1.529×10^{-9}
580	5	1.36	19.1	0.76	1.534×10^{-9}
627	5	1.45	12.9	0.645	1.729×10^{-8}
637	5	1.54	16.5	0.825	1.804×10^{-8}
647	5	2.0	17.8	0.89	1.905×10^{-8}

The migrating liquid film thickness,(δ), after 5 s and 10 s was measured at 1000X magnification with the help of a reticule consisting of graduated measuring scale and are given in table 3.8 at different temperatures. Growth distance was measured at the same instance for the same liquid film for which the thickness has been measured to calculate the growth rate by $\frac{nx}{t}$. Where n is the slope obtained from Fig. 3.18.

As can be seen from table 3.8, the thickness (δ) of the liquid film decreases with the increase in temperature of treatment for down- quenching experiment and liquid film thickness increases with increase in temperature of treatment for up-quenching experiment, consistent with calculated effective diffusive distance, D_v/v values which increase with increase in temperature of anneal. The diffusion coefficient of Cu in liquid film at different temperatures of up and down-quenching experiments has been calculated by the following equation given by Brechet and Purdy [24] and were shown in table 3.8.

$$D_L = \frac{vX_B^S(1-k)\delta}{k\Delta X_B} m^2 s^{-1} \qquad (13)$$

where k is the distribution coefficient, X_B^S is the atom fraction of Cu in the alloyed zone. The values of D_L were plotted in an Arhenius graph of ln D_L vs. 1/T, for down-quenching experiments in Fig.3.25, for up-quenching experiments in Fig.3.26, where T is in K. The data points fall on a straight line within the error of the experimental values. The activation energy has been calculated from the slope of the line, with a value of 45 kJ mol^{-1}. In comparison the activation energy of self diffusion in liquid Al has been reported [15] to be 38 kJ mol^{-1} and that of Cu in liquid Cu has been reported to be 40.7 kJ mol^{-1}. The diffusion of Cu in liquid Al is expected to lie within these values. The experimentally observed value is within ±10 kJ mol^{-1}. It can be concluded that the liquid film migration during down-quench experiment is controlled by the diffusion of Cu atoms in liquid Al.

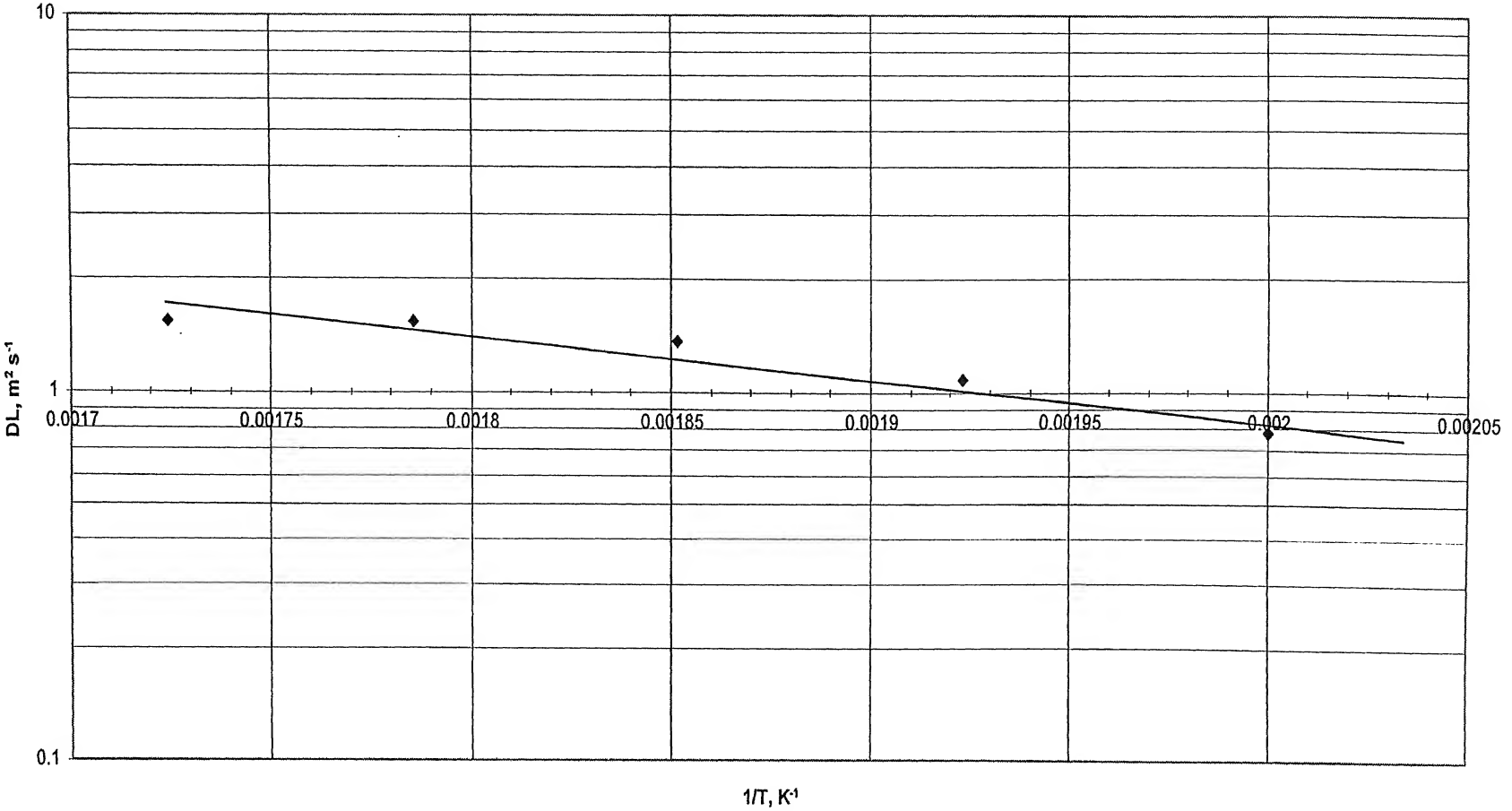

Fig.3.25 Plot of 1/T vs log D_L for down-quenching experiments.

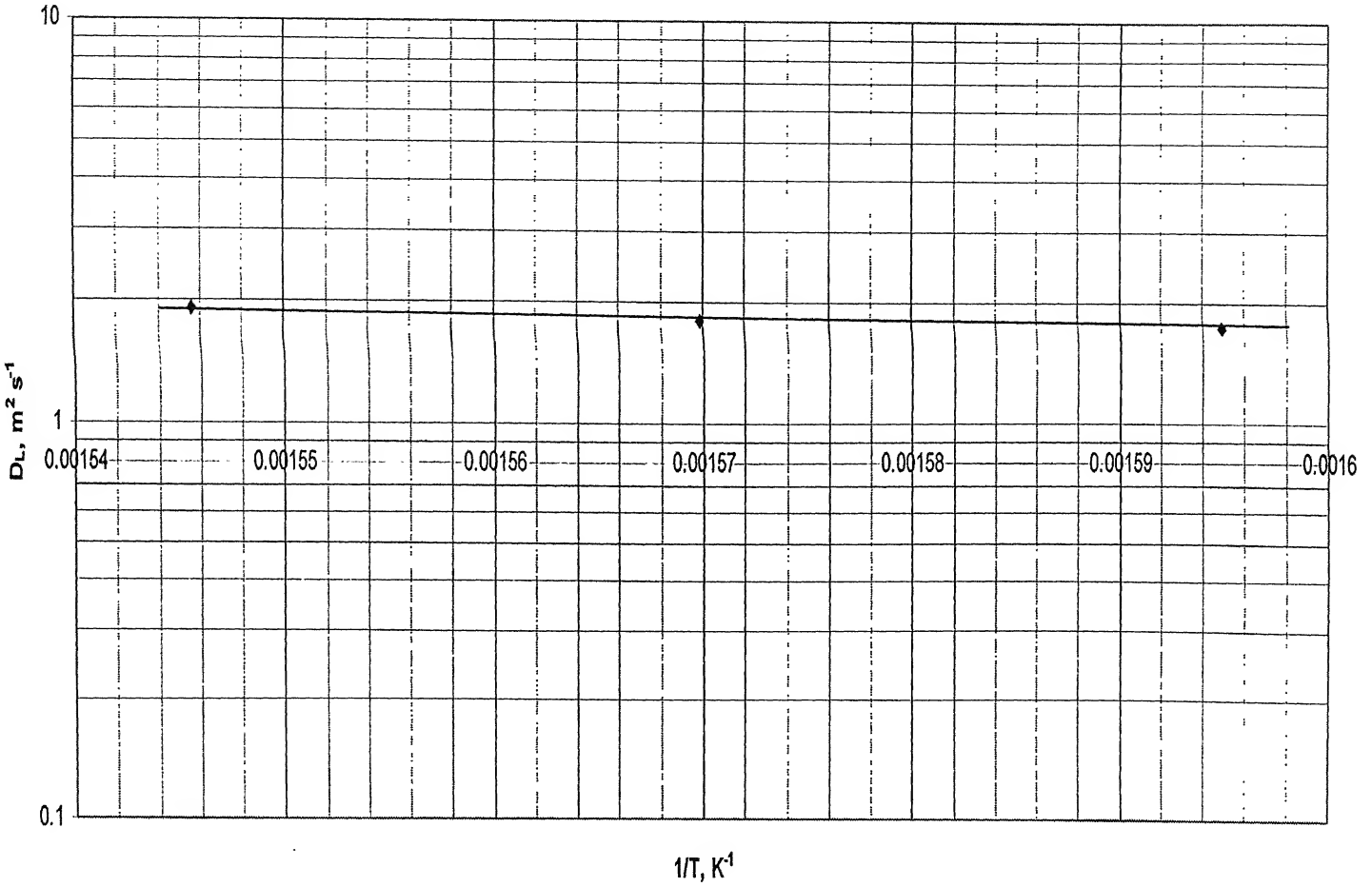

Fig.3.26. Plot 1/T vs log D_L for up-quenching experiments.

4. Conclusions

- When a chemical instability is introduced by a temperature change, the boundary migration occurred.
- The distance of migration of the grain boundary has been observed to increase with increasing time of anneal but the rate of migration has been found to decrease with the increasing time of anneal in both up and down-quenching experiments.
- Sufficient penetration of Cu in to the lattice ahead of migrating liquid film has been observed at all temperatures of experiment to ensure development of a coherently strained layer.
- Coherency strain energy is just not sufficient to cause migration; chemical free energy change is the driving force for the migration of liquid film.
- The growth velocity was observed to decrease with increasing time of diffusion anneal. This may be due to the reduced driving force associated with dissolution or growth of homogeneous liquid globules leading to change in composition ahead of migrating liquid film.
- Cu concentration difference across the liquid film is in the order of 10^{-4}, and the difference decreases as the temperature is increased.
- Liquid film migration during up and down-quenching experiments is controlled by the diffusion of Cu atoms in liquid Al.

5. References

1) D.N. Yoon and W.J. Huppmann; Acta metall., 1979, 27, 973.
2) J.Y. Baik and D.N. Yoon; Acta metall., 1985, 33, 1911.
3) E.P. Butler and A.H. Heuer; J. Am. Ceram. Soc., 1985, 68, 197.
4) W.A. Owczarski, D.S. Duvall and C.P. Sullivan; Weld. J., 1966, 45, 145.
5) M.S. Sulonen; Ann. Acad. Sci. Fenn. A. 1957, 1, 1-68.
6) M. Hillert; Metall. Trans., 1972, 3A, 2729-2741.
7) D.N. Yoon, J.W. Cahn, C.A. Handwerker, J.E. Blendell and Y.J. Baik; Interface migration and control of microstructure, eds C.S. Pande, A.H. King and J. Walter, ASM Int., Metals Park, Ohio, 1986, p. 19.
8) C.A. Handwerker, J.W. Cahn, D.N. Yoon and J.E. Blendell., Diffusion in solids: Recent Developments, ed. M.A. Dayananda and G.E. Murch. Metall. Soc. Of AIME, Warrendale, Pa. 1985, p. 275.
9) F.C. Larché and J.W. Cahn; Acta metall., 1985, 33, 331.
10) J.W. Cahn; Acta mëtall., 1961, 9, 795.
11) M. Hillert; Scripta metal., 1983, 17, 237.
12) R.A. Fournelle; Mater. Sci. Eng., A138, 133, 1991.
13) J.L. Murray; Intl. Metall. Rev., 30, 211, 1985.
14) Kaufman and Nesor from ref. [13]
15) T. Owadano, N. Ofuchi and K. Yusa, Kyushu Kogyo Krigaku Kenkyu Hokuku Kugaku, 22, 45, 1971.
16) N.A. Gjostein, in Diffusion, p. 241. Am. Soc. Metals, Metals Park, Ohio, 1973.
17) M. Hillert, in Lectures on the theory of phase transformations, H. Aarronson, editor, AIME.
18) D.Y. Yoon; Theories and observations of chemically induced interface migration, Intl. Mater. Rev., 40, 4, 1995.
19) M. Kuo and R.A. Fournelle; Acta metall.,39, 11, 2835-2845, 1991.
20) F. Fukikawa and K. Hirano, DIMETA 88, Proc. Intl. Conf. in metals and alloys, Eds. F.J. Kedves and D.L. Beke; Defect and Diffusion Forum, 1989, 66-69, 447.
21) P.M. Sutton; Phy. Rev., 91, 816, 1953.

22) Pearson and William Burton; Handbook of lattice spacings and structures of metals and alloys, Intl. series of monographs on metal physics and physical metallurgy, vol.4.

23) M. Gunduz and J.D. Hunt; Acta metal., 33, 1651, 1985.

24) Y. Brechet and G.R. Purdy; Scr. Metall., 22, 1629-1633, 1988.

A 148396

Date Slip

This book is to be returned on the date last stamped.

.....	.....
.....	.....
.....	.....
.....	.....
.....	.....
.....	.....
.....	.....
.....	.....
.....	.....
.....	.....
.....	.....
.....	.....